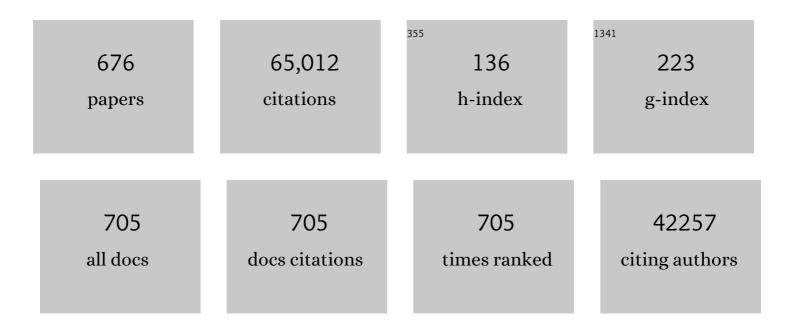
List of Publications by Year in descending order

Source: https://exaly.com/author-pdf/5357422/publications.pdf Version: 2024-02-01



MEILIN LIU

#	Article	IF	CITATIONS
1	Metal–Air Batteries with High Energy Density: Li–Air versus Zn–Air. Advanced Energy Materials, 2011, 1, 34-50.	10.2	1,906
2	A review on fundamentals and applications of electrophoretic deposition (EPD). Progress in Materials Science, 2007, 52, 1-61.	16.0	1,807
3	Nickel–Cobalt Hydroxide Nanosheets Coated on NiCo ₂ O ₄ Nanowires Grown on Carbon Fiber Paper for High-Performance Pseudocapacitors. Nano Letters, 2013, 13, 3135-3139.	4.5	992
4	Enhanced Sulfur and Coking Tolerance of a Mixed Ion Conductor for SOFCs: BaZr _{0.1} Ce _{0.7} Y _{0.2–} <i> _x </i> Yb <i> _x </i> O _{3–Î} . Science, 2009, 326, 126-129.	6.0	954
5	Facile Synthesis of Nitrogenâ€Doped Graphene via Pyrolysis of Graphene Oxide and Urea, and its Electrocatalytic Activity toward the Oxygenâ€Reduction Reaction. Advanced Energy Materials, 2012, 2, 884-888.	10.2	840
6	Fiber Supercapacitors Made of Nanowireâ€Fiber Hybrid Structures for Wearable/Flexible Energy Storage. Angewandte Chemie - International Edition, 2011, 50, 1683-1687.	7.2	796
7	Recent developments in heterogeneous photocatalytic water treatment using visible light-responsive photocatalysts: a review. RSC Advances, 2015, 5, 14610-14630.	1.7	796
8	Chemical reduction of three-dimensional silica micro-assemblies into microporous silicon replicas. Nature, 2007, 446, 172-175.	13.7	727
9	Enhancing SOFC cathode performance by surface modification through infiltration. Energy and Environmental Science, 2014, 7, 552.	15.6	680
10	Recent Progress in Nonâ€Precious Catalysts for Metalâ€Air Batteries. Advanced Energy Materials, 2012, 2, 816-829.	10.2	652
11	Enhancing Electrocatalytic Activity of Perovskite Oxides by Tuning Cation Deficiency for Oxygen Reduction and Evolution Reactions. Chemistry of Materials, 2016, 28, 1691-1697.	3.2	635
12	Promotion of oxygen reduction by a bio-inspired tethered iron phthalocyanine carbon nanotube-based catalyst. Nature Communications, 2013, 4, 2076.	5.8	630
13	Ba(Zr0.1Ce0.7Y0.2)O3–δas an Electrolyte for Low-Temperature Solid-Oxide Fuel Cells. Advanced Materials, 2006, 18, 3318-3320.	11.1	587
14	Sm0.5Sr0.5CoO3 cathodes for low-temperature SOFCs. Solid State Ionics, 2002, 149, 11-19.	1.3	576
15	Nanoporous Structures Prepared by an Electrochemical Deposition Process. Advanced Materials, 2003, 15, 1610-1614.	11.1	551
16	A comprehensive review of Li4Ti5O12-based electrodes for lithium-ion batteries: The latest advancements and future perspectives. Materials Science and Engineering Reports, 2015, 98, 1-71.	14.8	501
17	Hierarchical Network Architectures of Carbon Fiber Paper Supported Cobalt Oxide Nanonet for High-Capacity Pseudocapacitors. Nano Letters, 2012, 12, 321-325.	4.5	500
18	Flexible Zn– and Li–air batteries: recent advances, challenges, and future perspectives. Energy and Environmental Science, 2017, 10, 2056-2080.	15.6	477

#	Article	IF	CITATIONS
19	Nanostructured electrodes for lithium-ion and lithium-air batteries: the latest developments, challenges, and perspectives. Materials Science and Engineering Reports, 2011, 72, 203-252.	14.8	467
20	SnS nanoparticles electrostatically anchored on three-dimensional N-doped graphene as an active and durable anode for sodium-ion batteries. Energy and Environmental Science, 2017, 10, 1757-1763.	15.6	431
21	A Perovskite Electrocatalyst for Efficient Hydrogen Evolution Reaction. Advanced Materials, 2016, 28, 6442-6448.	11.1	429
22	Copper Foam Structures with Highly Porous Nanostructured Walls. Chemistry of Materials, 2004, 16, 5460-5464.	3.2	413
23	Three-dimensional ultrathin Ni(OH)2 nanosheets grown on nickel foam for high-performance supercapacitors. Nano Energy, 2015, 11, 154-161.	8.2	379
24	A Perovskite Nanorod as Bifunctional Electrocatalyst for Overall Water Splitting. Advanced Energy Materials, 2017, 7, 1602122.	10.2	369
25	3D Nitrogen-doped graphene prepared by pyrolysis of graphene oxide with polypyrrole for electrocatalysis of oxygen reduction reaction. Nano Energy, 2013, 2, 241-248.	8.2	367
26	Controlled synthesis of NiCo2S4 nanostructured arrays on carbon fiber paper for high-performance pseudocapacitors. Nano Energy, 2015, 16, 71-80.	8.2	354
27	High-Performance Energy Storage and Conversion Materials Derived from a Single Metal–Organic Framework/Graphene Aerogel Composite. Nano Letters, 2017, 17, 2788-2795.	4.5	348
28	Enhancing Sodium Ion Battery Performance by Strongly Binding Nanostructured Sb ₂ S ₃ on Sulfur-Doped Graphene Sheets. ACS Nano, 2016, 10, 10953-10959.	7.3	344
29	Effect of particle size and dopant on properties of SnO2-based gas sensors. Sensors and Actuators B: Chemical, 2000, 69, 144-152.	4.0	341
30	Markedly Enhanced Oxygen Reduction Activity of Single-Atom Fe Catalysts via Integration with Fe Nanoclusters. ACS Nano, 2019, 13, 11853-11862.	7.3	340
31	Three-Dimensional Porous Copper-Tin Alloy Electrodes for Rechargeable Lithium Batteries. Advanced Functional Materials, 2005, 15, 582-586.	7.8	339
32	Simple preparation of nanoporous few-layer nitrogen-doped graphene for use as an efficient electrocatalyst for oxygen reduction and oxygen evolution reactions. Carbon, 2013, 53, 130-136.	5.4	331
33	Nanoscale Surface Modification of Lithiumâ€Rich Layeredâ€Oxide Composite Cathodes for Suppressing Voltage Fade. Angewandte Chemie - International Edition, 2015, 54, 13058-13062.	7.2	331
34	Nickel-based pillared MOFs for high-performance supercapacitors: Design, synthesis and stability study. Nano Energy, 2016, 26, 66-73.	8.2	330
35	Harnessing the concurrent reaction dynamics in active Si and Ge to achieve high performance lithium-ion batteries. Energy and Environmental Science, 2018, 11, 669-681.	15.6	329
36	A tailored double perovskite nanofiber catalyst enables ultrafast oxygen evolution. Nature Communications, 2017, 8, 14586.	5.8	327

#	Article	IF	CITATIONS
37	A Highly Efficient Electrocatalyst for the Oxygen Reduction Reaction: Nâ€Doped Ketjenblack Incorporated into Fe/Fe ₃ Câ€Functionalized Melamine Foam. Angewandte Chemie - International Edition, 2013, 52, 1026-1030.	7.2	324
38	A Highly Sensitive and Fast-Responding SnO2 Sensor Fabricated by Combustion Chemical Vapor Deposition. Chemistry of Materials, 2005, 17, 3997-4000.	3.2	317
39	A Novel Composite Cathode for Lowâ€Temperature SOFCs Based on Oxide Proton Conductors. Advanced Materials, 2008, 20, 3280-3283.	11.1	314
40	Low-temperature SOFCs based on Gd0.1Ce0.9O1.95 fabricated by dry pressing. Solid State Ionics, 2001, 144, 249-255.	1.3	313
41	Enhancing Electrocatalytic Activity for Hydrogen Evolution by Strongly Coupled Molybdenum Nitride@Nitrogen-Doped Carbon Porous Nano-Octahedrons. ACS Catalysis, 2017, 7, 3540-3547.	5.5	306
42	Dramatically enhanced reversibility of Li ₂ O in SnO ₂ -based electrodes: the effect of nanostructure on high initial reversible capacity. Energy and Environmental Science, 2016, 9, 595-603.	15.6	300
43	Self-Assembled Triple-Conducting Nanocomposite as a Superior Protonic Ceramic Fuel Cell Cathode. Joule, 2019, 3, 2842-2853.	11.7	292
44	Germanium Nanotubes Prepared by Using the Kirkendall Effect as Anodes for Highâ€Rate Lithium Batteries. Angewandte Chemie - International Edition, 2011, 50, 9647-9650.	7.2	288
45	Highly efficient and robust cathode materials for low-temperature solid oxide fuel cells: PrBa0.5Sr0.5Co2â^'xFexO5+l´. Scientific Reports, 2013, 3, 2426.	1.6	285
46	Promotion of water-mediated carbon removal by nanostructured barium oxide/nickel interfaces in solid oxide fuel cells. Nature Communications, 2011, 2, 357.	5.8	280
47	From Ni-YSZ to sulfur-tolerant anode materials for SOFCs: electrochemical behavior, in situ characterization, modeling, and future perspectives. Energy and Environmental Science, 2011, 4, 4380.	15.6	280
48	Anion and cation substitution in transition-metal oxides nanosheets for high-performance hybrid supercapacitors. Nano Energy, 2019, 57, 22-33.	8.2	279
49	A Lowâ€Cost, Selfâ€Standing NiCo ₂ O ₄ @CNT/CNT Multilayer Electrode for Flexible Asymmetric Solidâ€State Supercapacitors. Advanced Functional Materials, 2017, 27, 1702160.	7.8	277
50	V ₅ S ₈ –graphite hybrid nanosheets as a high rate-capacity and stable anode material for sodium-ion batteries. Energy and Environmental Science, 2017, 10, 107-113.	15.6	274
51	Construction of MoS ₂ /C Hierarchical Tubular Heterostructures for High-Performance Sodium Ion Batteries. ACS Nano, 2018, 12, 12578-12586.	7.3	272
52	Rational SOFC material design: new advances and tools. Materials Today, 2011, 14, 534-546.	8.3	263
53	Densely Populated Isolated Single CoN Site for Efficient Oxygen Electrocatalysis. Advanced Energy Materials, 2019, 9, 1900149.	10.2	262
54	Ketjenblack Carbon Supported Amorphous Manganese Oxides Nanowires as Highly Efficient Electrocatalyst for Oxygen Reduction Reaction in Alkaline Solutions. Nano Letters, 2011, 11, 5362-5366.	4.5	261

#	Article	IF	CITATIONS
55	Facile preparation of nitrogen-doped graphene as a metal-free catalyst for oxygen reduction reaction. Physical Chemistry Chemical Physics, 2012, 14, 3381.	1.3	261
56	A New rGOâ€Overcoated Sb ₂ Se ₃ Nanorods Anode for Na ⁺ Battery: In Situ Xâ€Ray Diffraction Study on a Live Sodiation/Desodiation Process. Advanced Functional Materials, 2017, 27, 1606242.	7.8	258
57	Tripleâ€Conducting Layered Perovskites as Cathode Materials for Protonâ€Conducting Solid Oxide Fuel Cells. ChemSusChem, 2014, 7, 2811-2815.	3.6	257
58	Anionic defect engineering of transition metal oxides for oxygen reduction and evolution reactions. Journal of Materials Chemistry A, 2019, 7, 5875-5897.	5.2	252
59	Achieving Fast and Durable Lithium Storage through Amorphous FeP Nanoparticles Encapsulated in Ultrathin 3D P-Doped Porous Carbon Nanosheets. ACS Nano, 2020, 14, 9545-9561.	7.3	250
60	A Highâ€Performance Electrocatalyst for Oxygen Evolution Reaction: LiCo _{0.8} Fe _{0.2} O ₂ . Advanced Materials, 2015, 27, 7150-7155.	11.1	249
61	Controlling cation segregation in perovskite-based electrodes for high electro-catalytic activity and durability. Chemical Society Reviews, 2017, 46, 6345-6378.	18.7	246
62	Novel Cathodes for Low-Temperature Solid Oxide Fuel Cells. Advanced Materials, 2002, 14, 521-523.	11.1	243
63	Anomalous Pseudocapacitive Behavior of a Nanostructured, Mixed-Valent Manganese Oxide Film for Electrical Energy Storage. Nano Letters, 2012, 12, 3483-3490.	4.5	234
64	A high-performance supercapacitor electrode based on N-doped porous graphene. Journal of Power Sources, 2018, 387, 43-48.	4.0	231
65	MOF-derived α-NiS nanorods on graphene as an electrode for high-energy-density supercapacitors. Journal of Materials Chemistry A, 2018, 6, 4003-4012.	5.2	231
66	A robust fuel cell operated on nearly dry methane at 500 °C enabled by synergistic thermal catalysis and electrocatalysis. Nature Energy, 2018, 3, 1042-1050.	19.8	230
67	Advances in Cathode Materials for Solid Oxide Fuel Cells: Complex Oxides without Alkaline Earth Metal Elements. Advanced Energy Materials, 2015, 5, 1500537.	10.2	229
68	Design and understanding of dendritic mixed-metal hydroxide nanosheets@N-doped carbon nanotube array electrode for high-performance asymmetric supercapacitors. Energy Storage Materials, 2019, 16, 632-645.	9.5	225
69	A Highly Efficient Multi-phase Catalyst Dramatically Enhances the Rate of Oxygen Reduction. Joule, 2018, 2, 938-949.	11.7	221
70	Sulfur Poisoning and Regeneration of Ni-Based Anodes in Solid Oxide Fuel Cells. Journal of the Electrochemical Society, 2007, 154, B201.	1.3	217
71	Mechanistic Origin of the High Performance of Yolk@Shell Bi ₂ S ₃ @N-Doped Carbon Nanowire Electrodes. ACS Nano, 2018, 12, 12597-12611.	7.3	213
72	Probing the Charge Storage Mechanism of a Pseudocapacitive MnO ₂ Electrode Using <i>in Operando</i> Raman Spectroscopy. Chemistry of Materials, 2015, 27, 6608-6619.	3.2	212

#	Article	IF	CITATIONS
73	Bigger is Surprisingly Better: Agglomerates of Larger RuP Nanoparticles Outperform Benchmark Pt Nanocatalysts for the Hydrogen Evolution Reaction. Advanced Materials, 2018, 30, e1800047.	11.1	212
74	Controlled synthesis of three-phase NixSy/rGO nanoflake electrodes for hybrid supercapacitors with highÂenergy and power density. Nano Energy, 2017, 33, 522-531.	8.2	211
75	Rational Design of Nickel Hydroxideâ€Based Nanocrystals on Graphene for Ultrafast Energy Storage. Advanced Energy Materials, 2018, 8, 1702247.	10.2	211
76	Hybrid-solid oxide electrolysis cell: A new strategy for efficient hydrogen production. Nano Energy, 2018, 44, 121-126.	8.2	209
77	Characterization of sulfur poisoning of Ni–YSZ anodes for solid oxide fuel cells using in situ Raman microspectroscopy. Solid State Ionics, 2007, 178, 925-935.	1.3	206
78	Fabrication of SnS ₂ /Mn ₂ SnS ₄ /Carbon Heterostructures for Sodium-Ion Batteries with High Initial Coulombic Efficiency and Cycling Stability. ACS Nano, 2019, 13, 3666-3676.	7.3	205
79	A robust and active hybrid catalyst for facile oxygen reduction in solid oxide fuel cells. Energy and Environmental Science, 2017, 10, 964-971.	15.6	204
80	Promotion of Oxygen Reduction by Exsolved Silver Nanoparticles on a Perovskite Scaffold for Low-Temperature Solid Oxide Fuel Cells. Nano Letters, 2016, 16, 512-518.	4.5	202
81	Engineering phosphorus-doped LaFeO3-δ perovskite oxide as robust bifunctional oxygen electrocatalysts in alkaline solutions. Nano Energy, 2018, 47, 199-209.	8.2	202
82	A highly active, CO ₂ -tolerant electrode for the oxygen reduction reaction. Energy and Environmental Science, 2018, 11, 2458-2466.	15.6	202
83	Raman Spectroscopy of Nickel Sulfide Ni ₃ S ₂ . Journal of Physical Chemistry C, 2007, 111, 17997-18000.	1.5	195
84	Phase evolution of an alpha MnO 2 -based electrode for pseudo-capacitors probed by in operando Raman spectroscopy. Nano Energy, 2014, 9, 161-167.	8.2	195
85	Promotion of Proton Conduction in Polymer Electrolyte Membranes by 1H-1,2,3-Triazole. Journal of the American Chemical Society, 2005, 127, 10824-10825.	6.6	193
86	Reduced-Temperature Solid Oxide Fuel Cells Fabricated by Screen Printing. Electrochemical and Solid-State Letters, 2001, 4, A52.	2.2	192
87	Boosting Oxygen Evolution Reaction by Creating Both Metal Ion and Latticeâ€Oxygen Active Sites in a Complex Oxide. Advanced Materials, 2020, 32, e1905025.	11.1	190
88	Crosslinking Graphene Oxide into Robust 3D Porous Nâ€Đoped Graphene. Advanced Materials, 2015, 27, 5171-5175.	11.1	188
89	Unusual synergistic effect in layered Ruddlesdenâ^'Popper oxide enables ultrafast hydrogen evolution. Nature Communications, 2019, 10, 149.	5.8	187
90	Lithium-Doping Stabilized High-Performance P2–Na _{0.66} Li _{0.18} Fe _{0.12} Mn _{0.7} O ₂ Cathode for Sodium Ion Batteries. Journal of the American Chemical Society, 2019, 141, 6680-6689.	6.6	187

#	Article	IF	CITATIONS
91	Densely Populated Single Atom Catalysts. Small Methods, 2020, 4, 1900540.	4.6	185
92	Atomically dispersed Fe–N–C decorated with Pt-alloy core–shell nanoparticles for improved activity and durability towards oxygen reduction. Energy and Environmental Science, 2020, 13, 3032-3040.	15.6	185
93	Characterization of O2–CeO2 Interactions Using In Situ Raman Spectroscopy and First-Principle Calculations. ChemPhysChem, 2006, 7, 1957-1963.	1.0	184
94	Suppression of Sr surface segregation in La _{1â^'x} Sr _x Co _{1â^'y} Fe _y O _{3â^'δ} : a first principles study. Physical Chemistry Chemical Physics, 2013, 15, 489-496.	1.3	182
95	Hybrid Composite Ni(OH) ₂ @NiCo ₂ O ₄ Grown on Carbon Fiber Paper for High-Performance Supercapacitors. ACS Applied Materials & Interfaces, 2013, 5, 11159-11162.	4.0	181
96	Free-standing N-self-doped carbon nanofiber aerogels for high-performance all-solid-state supercapacitors. Nano Energy, 2019, 63, 103836.	8.2	178
97	Heterointerface engineering for enhancing the electrochemical performance of solid oxide cells. Energy and Environmental Science, 2020, 13, 53-85.	15.6	178
98	Porous Tin Oxides Prepared Using an Anodic Oxidation Process. Advanced Materials, 2004, 16, 237-240.	11.1	177
99	Photoelectron spectroscopy study of oxygen vacancy on vanadium oxides surface. Applied Surface Science, 2004, 236, 473-478.	3.1	177
100	Enhancement of La0.6Sr0.4Co0.2Fe0.8O3-δ durability and surface electrocatalytic activity by La0.85Sr0.15MnO3±δ investigated using a new test electrode platform. Energy and Environmental Science, 2011, 4, 2249.	15.6	176
101	Chemically activated hollow carbon nanospheres as a high-performance anode material for potassium ion batteries. Journal of Materials Chemistry A, 2018, 6, 24317-24323.	5.2	174
102	La0.6Sr0.4Co0.2Fe0.8O3â^'δ cathodes infiltrated with samarium-doped cerium oxide for solid oxide fuel cells. Journal of Power Sources, 2010, 195, 4704-4708.	4.0	173
103	In situ fabrication of CoFe alloy nanoparticles structured (Pr0.4Sr0.6)3(Fe0.85Nb0.15)2O7 ceramic anode for direct hydrocarbon solid oxide fuel cells. Nano Energy, 2015, 11, 704-710.	8.2	173
104	High-performance hybrid supercapacitors based on self-supported 3D ultrathin porous quaternary Zn-Ni-Al-Co oxide nanosheets. Nano Energy, 2016, 28, 475-485.	8.2	173
105	Well-Aligned"Nano-Box-Beams―of SnO2. Advanced Materials, 2004, 16, 353-356.	11.1	171
106	Unraveling the Nature of Anomalously Fast Energy Storage in T-Nb ₂ O ₅ . Journal of the American Chemical Society, 2017, 139, 7071-7081.	6.6	171
107	A solid oxide fuel cell operating on hydrogen sulfide (H2S) and sulfur-containing fuels. Journal of Power Sources, 2004, 135, 17-24.	4.0	170
108	Woodâ€Derived Hierarchically Porous Electrodes for Highâ€Performance Allâ€Solidâ€State Supercapacitors. Advanced Functional Materials, 2018, 28, 1806207.	7.8	170

#	Article	IF	CITATIONS
109	Electrical properties and sulfur tolerance of La0.75Sr0.25Cr1â^'xMnxO3 under anodic conditions. Journal of Solid State Chemistry, 2005, 178, 1844-1850.	1.4	169
110	Functionalized Bimetallic Hydroxides Derived from Metal–Organic Frameworks for High-Performance Hybrid Supercapacitor with Exceptional Cycling Stability. ACS Energy Letters, 2017, 2, 1263-1269.	8.8	167
111	Growth of Aligned Square-Shaped SnO2 Tube Arrays. Advanced Functional Materials, 2005, 15, 57-62.	7.8	165
112	A mixed proton, oxygen ion, and electron conducting cathode for SOFCs based on oxide proton conductors. Journal of Power Sources, 2010, 195, 471-474.	4.0	164
113	Crystallinity Dependence of Ruthenium Nanocatalyst toward Hydrogen Evolution Reaction. ACS Catalysis, 2018, 8, 5714-5720.	5.5	162
114	Recent Progress in Electrocatalysts for Acidic Water Oxidation. Advanced Energy Materials, 2020, 10, 2000478.	10.2	162
115	Enhanced performance of LSCF cathode through surface modification. International Journal of Hydrogen Energy, 2012, 37, 8613-8620.	3.8	161
116	Nitrogen-doped bamboo-like carbon nanotubes as anode material for high performance potassium ion batteries. Journal of Materials Chemistry A, 2018, 6, 15162-15169.	5.2	161
117	Novel Solid Redox Polymerization Electrodes: All‣olid‣tate, Thinâ€Film, Rechargeable Lithium Batteries. Journal of the Electrochemical Society, 1991, 138, 1891-1895.	1.3	160
118	A high-performance anode for lithium ion batteries: Fe ₃ O ₄ microspheres encapsulated in hollow graphene shells. Journal of Materials Chemistry A, 2015, 3, 11847-11856.	5.2	159
119	A high-energy, long cycle-life hybrid supercapacitor based on graphene composite electrodes. Energy Storage Materials, 2017, 7, 32-39.	9.5	157
120	Woodâ€Derived Materials for Advanced Electrochemical Energy Storage Devices. Advanced Functional Materials, 2019, 29, 1902255.	7.8	157
121	Oxygen- and Nitrogen-Enriched 3D Porous Carbon for Supercapacitors of High Volumetric Capacity. ACS Applied Materials & Interfaces, 2015, 7, 24622-24628.	4.0	156
122	In situ X-ray diffraction characterization of NiSe2 as a promising anode material for sodium ion batteries. Journal of Power Sources, 2017, 343, 483-491.	4.0	155
123	Heterostructured Nanocubeâ€Shaped Binary Sulfide (SnCo)S ₂ Interlaced with Sâ€Doped Graphene as a Highâ€Performance Anode for Advanced Na ⁺ Batteries. Advanced Functional Materials, 2019, 29, 1807971.	7.8	154
124	Core-shell structured Fe2O3@Fe3C@C nanochains and Ni–Co carbonate hydroxide hybridized microspheres for high-performance battery-type supercapacitor. Journal of Power Sources, 2021, 482, 228915.	4.0	153
125	Improving the Activity for Oxygen Evolution Reaction by Tailoring Oxygen Defects in Double Perovskite Oxides. Advanced Functional Materials, 2019, 29, 1901783.	7.8	152
126	Porous silicon negative electrodes for rechargeable lithium batteries. Journal of Power Sources, 2005, 139, 314-320.	4.0	151

#	Article	IF	CITATIONS
127	Heterointerface Engineering of Hierarchical Bi ₂ S ₃ /MoS ₂ with Selfâ€Generated Rich Phase Boundaries for Superior Sodium Storage Performance. Advanced Functional Materials, 2020, 30, 1910732.	7.8	151
128	A robust sulfur host with dual lithium polysulfide immobilization mechanism for long cycle life and high capacity Li-S batteries. Energy Storage Materials, 2019, 16, 344-353.	9.5	150
129	Recent progress in the design of metal sulfides as anode materials for sodium ion batteries. Energy Storage Materials, 2019, 22, 66-95.	9.5	149
130	X-ray photoelectron spectroscopy of La0.5Sr0.5MnO3. Materials Letters, 2005, 59, 1980-1983.	1.3	145
131	1H-1,2,4-Triazole:  An Effective Solvent for Proton-Conducting Electrolytes. Chemistry of Materials, 2005, 17, 5884-5886.	3.2	144
132	Efficient Electro atalysts for Enhancing Surface Activity and Stability of SOFC Cathodes. Advanced Energy Materials, 2013, 3, 1149-1154.	10.2	144
133	A Theoretical Study of Surface Reduction Mechanisms of CeO2(111) and (110) by H2. ChemPhysChem, 2007, 8, 849-855.	1.0	142
134	MoS ₂ -covered SnS nanosheets as anode material for lithium-ion batteries with high capacity and long cycle life. Journal of Materials Chemistry A, 2018, 6, 592-598.	5.2	142
135	Designing and Understanding the Superior Potassium Storage Performance of Nitrogen/Phosphorus Coâ€Doped Hollow Porous Bowlâ€Like Carbon Anodes. Advanced Functional Materials, 2021, 31, .	7.8	142
136	Fabrication and modification of solid oxide fuel cell anodes via wet impregnation/infiltration technique. Journal of Power Sources, 2013, 237, 243-259.	4.0	140
137	Chemically Stable Yttrium and Tin Coâ€Doped Barium Zirconate Electrolyte for Next Generation High Performance Protonâ€Conducting Solid Oxide Fuel Cells. Advanced Energy Materials, 2013, 3, 1041-1050.	10.2	140
138	Effect of Zr-Doping on the Chemical Stability and Hydrogen Permeation of the Niâ^'BaCe0.8Y0.2O3-αMixed Protonicâ^'Electronic Conductor. Chemistry of Materials, 2006, 18, 4647-4650.	3.2	139
139	Defect Engineering in Single-Layer MoS ₂ Using Heavy Ion Irradiation. ACS Applied Materials & Interfaces, 2018, 10, 42524-42533.	4.0	138
140	Microstructures, conductivities, and electrochemical properties of Ce0.9Gd0.1O2 and GDC–Ni anodes for low-temperature SOFCs. Solid State Ionics, 2002, 152-153, 423-430.	1.3	137
141	MoS 2 encapsulated SnO 2 -SnS/C nanosheets as a high performance anode material for lithium ion batteries. Chemical Engineering Journal, 2017, 316, 393-400.	6.6	136
142	Uncovering the Effect of Lattice Strain and Oxygen Deficiency on Electrocatalytic Activity of Perovskite Cobaltite Thin Films. Advanced Science, 2019, 6, 1801898.	5.6	136
143	Electrochemical Properties of Organic Disulfide/Thiolate Redox Couples. Journal of the Electrochemical Society, 1989, 136, 2570-2575.	1.3	135
144	Title is missing!. Journal of Materials Science, 1999, 34, 3213-3219.	1.7	133

#	Article	IF	CITATIONS
145	Co ₃ O ₄ Nanosheets as Active Material for Hybrid Zn Batteries. Small, 2018, 14, e1800225.	5.2	131
146	Identification of nickel sulfides on Ni–YSZ cermet exposed to H2 fuel containing H2S using Raman spectroscopy. Journal of Power Sources, 2006, 156, 461-465.	4.0	129
147	Recent Advances in Perovskite Oxides as Electrode Materials for Nonaqueous Lithium–Oxygen Batteries. Advanced Energy Materials, 2017, 7, 1602674.	10.2	129
148	Influence of cell voltage and current on sulfur poisoning behavior of solid oxide fuel cells. Journal of Power Sources, 2007, 172, 688-693.	4.0	128
149	Progress and Prospects in Symmetrical Solid Oxide Fuel Cells with Two Identical Electrodes. Advanced Energy Materials, 2015, 5, 1500188.	10.2	128
150	Preparation of yttria-stabilized zirconia (YSZ) films on La0.85Sr0.15MnO3 (LSM) and LSM–YSZ substrates using an electrophoretic deposition (EPD) process. Journal of the European Ceramic Society, 2001, 21, 127-134.	2.8	127
151	A Simple and Costâ€Effective Approach to Fabrication of Dense Ceramic Membranes on Porous Substrates. Journal of the American Ceramic Society, 2001, 84, 1903-1905.	1.9	127
152	DNA Functionalized Single-Walled Carbon Nanotubes for Electrochemical Detection. Journal of Physical Chemistry B, 2005, 109, 20072-20076.	1.2	127
153	Oxygen Reduction on LaMnO3-Based Cathode Materials in Solid Oxide Fuel Cells. Chemistry of Materials, 2007, 19, 1690-1699.	3.2	126
154	Ni-Ce0.9Gd0.1O1.95 anode for GDC electrolyte-based low-temperature SOFCs. Solid State Ionics, 2004, 166, 241-250.	1.3	125
155	Systematic study on structural and electronic properties of diamine/triamine functionalized graphene networks for supercapacitor application. Nano Energy, 2017, 31, 183-193.	8.2	124
156	Novel Nanostructured Electrodes for Solid Oxide Fuel Cells Fabricated by Combustion Chemical Vapor Deposition (CVD). Advanced Materials, 2004, 16, 256-260.	11.1	122
157	Suppressing dendrite growth by a functional electrolyte additive for robust Li metal anodes. Energy Storage Materials, 2019, 23, 701-706.	9.5	122
158	Computational study of sulfur–nickel interactions: A new S–Ni phase diagram. Electrochemistry Communications, 2007, 9, 2212-2217.	2.3	121
159	Preparation of mesoporous tin oxide for electrochemical applications. Chemical Communications, 1999, , 1829-1830.	2.2	120
160	Controllable interior structure of ZnCo2O4 microspheres for high-performance lithium-ion batteries. Nano Energy, 2015, 11, 64-70.	8.2	120
161	Effect of Interfacial Resistance on Determination of Transport Properties of Mixed onducting Electrolytes. Journal of the Electrochemical Society, 1996, 143, L109-L112.	1.3	119
162	Mixed tocopherols inhibit platelet aggregation in humans: potential mechanisms. American Journal of Clinical Nutrition, 2003, 77, 700-706.	2.2	118

#	Article	IF	CITATIONS
163	Direct octane fuel cells: A promising power for transportation. Nano Energy, 2012, 1, 448-455.	8.2	118
164	MOFs-derived porous Mo2C–C nano-octahedrons enable high-performance lithium–sulfur batteries. Energy Storage Materials, 2020, 25, 547-554.	9.5	118
165	Cobalt single atoms supported on N-doped carbon as an active and resilient sulfur host for lithium–sulfur batteries. Energy Storage Materials, 2020, 28, 196-204.	9.5	117
166	GDC-Based Low-Temperature SOFCs Powered by Hydrocarbon Fuels. Journal of the Electrochemical Society, 2004, 151, A1128.	1.3	116
167	Simultaneous Blockade of Both the Epidermal Growth Factor Receptor and the Insulin-like Growth Factor Receptor Signaling Pathways in Cancer Cells with a Fully Human Recombinant Bispecific Antibody. Journal of Biological Chemistry, 2004, 279, 2856-2865.	1.6	113
168	Improving La0.6Sr0.4Co0.2Fe0.8O3ⴴδ cathode performance by infiltration of a Sm0.5Sr0.5CoO3ⴴδ coating. Solid State Ionics, 2009, 180, 1285-1289.	1.3	112
169	In situ Raman study of nickel bicarbonate for high-performance energy storage device. Nano Energy, 2019, 64, 103919.	8.2	112
170	N/S codoped carbon microboxes with expanded interlayer distance toward excellent potassium storage. Chemical Engineering Journal, 2019, 358, 1147-1154.	6.6	112
171	Nanostructured Columnar Tin Oxide Thin Film Electrode for Lithium Ion Batteries. Chemistry of Materials, 2006, 18, 4643-4646.	3.2	111
172	A Scalable Freeâ€6tanding V ₂ O ₅ /CNT Film Electrode for Supercapacitors with a Wide Operation Voltage (1.6 V) in an Aqueous Electrolyte. Advanced Functional Materials, 2016, 26, 6114-6120.	7.8	109
173	Investigation into the origin of high stability of δ-MnO2 pseudo-capacitive electrode using operando Raman spectroscopy. Nano Energy, 2016, 30, 293-302.	8.2	109
174	A Highly Efficient and Robust Nanofiber Cathode for Solid Oxide Fuel Cells. Advanced Energy Materials, 2017, 7, 1601890.	10.2	109
175	An Active and Robust Air Electrode for Reversible Protonic Ceramic Electrochemical Cells. ACS Energy Letters, 0, , 1511-1520.	8.8	109
176	Electrode Kinetics of Organodisulfide Cathodes for Storage Batteries. Journal of the Electrochemical Society, 1990, 137, 750-759.	1.3	108
177	Composite Ni–Ba(Zr0.1Ce0.7Y0.2)O3 membrane for hydrogen separation. Journal of Power Sources, 2006, 159, 1291-1295.	4.0	108
178	Novel Solid Redox Polymerization Electrodes: Electrochemical Properties. Journal of the Electrochemical Society, 1991, 138, 1896-1901.	1.3	106
179	Raman spectroscopic monitoring of carbon deposition on hydrocarbon-fed solid oxide fuel cell anodes. Energy and Environmental Science, 2012, 5, 7913.	15.6	105
180	A Facile and Scalable Strategy for Fabrication of Superior Bifunctional Freestanding Air Electrodes for Flexible Zinc–Air Batteries. Advanced Functional Materials, 2020, 30, 2003407.	7.8	105

#	Article	IF	CITATIONS
181	Investigations into the origin of pseudocapacitive behavior of Mn ₃ O ₄ electrodes using in operando Raman spectroscopy. Journal of Materials Chemistry A, 2015, 3, 7338-7344.	5.2	104
182	Surface Modification of Na ₃ V ₂ (PO ₄) ₃ by Nitrogen and Sulfur Dual-Doped Carbon Layer with Advanced Sodium Storage Property. ACS Applied Materials & Interfaces, 2017, 9, 13151-13162.	4.0	103
183	Oxygen reduction reactions in the SOFC cathode of Ag/CeO2. Solid State Ionics, 2006, 177, 939-947.	1.3	101
184	Computational Study on the Catalytic Mechanism of Oxygen Reduction on La _{0.5} Sr _{0.5} MnO ₃ in Solid Oxide Fuel Cells. Angewandte Chemie - International Edition, 2007, 46, 7214-7219.	7.2	101
185	Electrochemical properties of Li–Mg alloy electrodes for lithium batteries. Journal of Power Sources, 2001, 92, 70-80.	4.0	100
186	Trapping sulfur in hierarchically porous, hollow indented carbon spheres: a high-performance cathode for lithium–sulfur batteries. Journal of Materials Chemistry A, 2016, 4, 9526-9535.	5.2	100
187	Design of TiO2eC hierarchical tubular heterostructures for high performance potassium ion batteries. Nano Energy, 2019, 59, 582-590.	8.2	100
188	In situ X-ray diffraction characterization of NbS2 nanosheets as the anode material for sodium ion batteries. Journal of Power Sources, 2016, 325, 410-416.	4.0	99
189	Synergistic Effect of Nitrogen and Sulfur Dualâ€Đoping Endows TiO ₂ with Exceptional Sodium Storage Performance. Advanced Energy Materials, 2021, 11, 2003037.	10.2	99
190	Electronic and vibrational properties of nickel sulfides from first principles. Journal of Chemical Physics, 2007, 127, 214705.	1.2	98
191	Construction and Performance Characterization of α-Fe ₂ O ₃ /rGO Composite for Long-Cycling-Life Supercapacitor Anode. ACS Sustainable Chemistry and Engineering, 2017, 5, 5067-5074.	3.2	98
192	Controlling the morphology and uniformity of a catalyst-infiltrated cathode for solid oxide fuel cells by tuning wetting property. Journal of Power Sources, 2010, 195, 419-424.	4.0	95
193	A durable, high-performance hollow-nanofiber cathode for intermediate-temperature fuel cells. Nano Energy, 2016, 26, 90-99.	8.2	93
194	Tuning proton-coupled electron transfer by crystal orientation for efficient water oxidization on double perovskite oxides. Nature Communications, 2020, 11, 4299.	5.8	93
195	Preparation of La _{1â^'<i>z</i>} Sr _{<i>z</i>} Co _{1â^'<i>y</i>} Fe _y O _{3â^'<i>xthin films, membranes, and coatings on dense and porous substrates. Journal of Materials Research, 1995. 10. 3210-3221.</i>}	> 1.2	92
196	Biomass-derived heteroatoms-doped mesoporous carbon for efficient oxygen reduction in microbial fuel cells. Biosensors and Bioelectronics, 2017, 98, 350-356.	5.3	92
197	A novel low-thermal-budget approach for the co-production of ethylene and hydrogen <i>via</i> the electrochemical non-oxidative deprotonation of ethane. Energy and Environmental Science, 2018, 11, 1710-1716.	15.6	92
198	Three-dimensional (3D) flower-like MoSe2/N-doped carbon composite as a long-life and high-rate anode material for sodium-ion batteries. Chemical Engineering Journal, 2019, 357, 226-236.	6.6	92

#	Article	IF	CITATIONS
199	Mesoporous catalytic filters for semiconductor gas sensors. Thin Solid Films, 2003, 436, 64-69.	0.8	91
200	Synthesis and gas sensing properties of ZnO single crystal flakes. Journal of Materials Chemistry, 2005, 15, 2316.	6.7	91
201	Rational Design of TiO–TiO ₂ Heterostructure/Polypyrrole as a Multifunctional Sulfur Host for Advanced Lithium–Sulfur Batteries. ACS Applied Materials & Interfaces, 2019, 11, 5055-5063.	4.0	91
202	Nanostructured and functionally graded cathodes for intermediate temperature solid oxide fuel cells. Journal of Power Sources, 2004, 138, 194-198.	4.0	90
203	Enhancing Electrode Performance by Exsolved Nanoparticles: A Superior Cobalt-Free Perovskite Electrocatalyst for Solid Oxide Fuel Cells. ACS Applied Materials & Interfaces, 2016, 8, 35308-35314.	4.0	90
204	Probing Structural Evolution and Charge Storage Mechanism of NiO ₂ H <i>_x</i> Electrode Materials using In Operando Resonance Raman Spectroscopy. Advanced Science, 2016, 3, 1500433.	5.6	90
205	Structure and surface chemistry of Al2O3 coated LiMn2O4 nanostructured electrodes with improved lifetime. Journal of Power Sources, 2016, 306, 162-170.	4.0	89
206	Facile Synthesis of a 3D Nanoarchitectured Li ₄ Ti ₅ O ₁₂ Electrode for Ultrafast Energy Storage. Advanced Energy Materials, 2016, 6, 1500924.	10.2	88
207	Perovskite SrCo _{0.9} Nb _{0.1} O _{3â^'<i>δ</i>} as an Anionâ€Intercalated Electrode Material for Supercapacitors with Ultrahigh Volumetric Energy Density. Angewandte Chemie - International Edition, 2016, 55, 9576-9579.	7.2	87
208	A New Family of Protonâ€Conducting Electrolytes for Reversible Solid Oxide Cells: BaHf <i>_x</i> Ce _{0.8â^'} <i>_x</i> Y _{0.1} Yb _{0.1} O <sub Advanced Functional Materials, 2020, 30, 2002265.</sub 	>3 â. 8 <td>›> ৰø≺sub>l´<</td>	›> ৰø ≺sub>l´<
209	Dual-Scale Porous Electrodes for Solid Oxide Fuel Cells from Polymer Foams. Advanced Materials, 2005, 17, 487-491.	11.1	85
210	Operando Investigation into Dynamic Evolution of Cathode–Electrolyte Interfaces in a Li-Ion Battery. Nano Letters, 2019, 19, 2037-2043.	4.5	85
211	Unraveling the high-activity nature of Fe–N–C electrocatalysts for the oxygen reduction reaction: the extraordinary synergy between Fe–N ₄ and Fe ₄ N. Journal of Materials Chemistry A, 2019, 7, 11792-11801.	5.2	84
212	Mesoporous Sn–TiO2 composite electrodes for lithium batteries. Chemical Communications, 2000, , 2125-2126.	2.2	83
213	Synthesis and Characterization of Self-Standing and Highly Flexible δ-MnO ₂ @CNTs/CNTs Composite Films for Direct Use of Supercapacitor Electrodes. ACS Applied Materials & Interfaces, 2016, 8, 23721-23728.	4.0	83
214	Nanoscale gadolinium doped ceria (GDC) surface modification of Li-rich layered oxide as a high performance cathode material for lithium ion batteries. Chemical Engineering Journal, 2018, 334, 497-507.	6.6	83
215	An In Situ Formed, Dualâ€Phase Cathode with a Highly Active Catalyst Coating for Protonic Ceramic Fuel Cells. Advanced Functional Materials, 2018, 28, 1704907.	7.8	82
216	Electrophoretic deposition on non-conducting substrates: The case of YSZ film on NiO–YSZ composite substrates for solid oxide fuel cell application. Journal of Power Sources, 2007, 173, 130-136.	4.0	81

#	Article	IF	CITATIONS
217	Ultrafine Pt nanoparticle-decorated robust 3D N-doped porous graphene as an enhanced electrocatalyst for methanol oxidation. Chemical Communications, 2016, 52, 382-385.	2.2	81
218	Transport properties of SrCe0.95Y0.05O3â^î´and its application for hydrogen separation. Solid State Ionics, 1998, 110, 303-310.	1.3	80
219	Functionally graded cathodes fabricated by sol-gel/slurry coating for honeycomb SOFCs. Solid State lonics, 2005, 176, 25-31.	1.3	80
220	Energy minimization with loop fusion and multi-functional-unit scheduling for multidimensional DSP. Journal of Parallel and Distributed Computing, 2008, 68, 443-455.	2.7	80
221	One-step synthesis of architectural Ni3S2 nanosheet-on-nanorods array for use as high-performance electrodes for supercapacitors. NPG Asia Materials, 2016, 8, e300-e300.	3.8	80
222	Fe _{1â^'x} S@S-doped carbon core–shell heterostructured hollow spheres as highly reversible anode materials for sodium ion batteries. Journal of Materials Chemistry A, 2019, 7, 20229-20238.	5.2	80
223	Equivalent Circuit Approximation to Porous Mixed onducting Oxygen Electrodes in Solid‧tate Cells. Journal of the Electrochemical Society, 1998, 145, 142-154.	1.3	79
224	Preparation of barium cerate-based thin films using a modified Pechini process. Journal of Materials Science, 1997, 32, 619-625.	1.7	78
225	Chemiluminescence from the Decomposition of Peroxymonocarbonate Catalyzed by Gold Nanoparticles. Journal of Physical Chemistry B, 2008, 112, 7850-7855.	1.2	78
226	Rational design of novel cathode materials in solid oxide fuel cells using first-principles simulations. Journal of Power Sources, 2010, 195, 1441-1445.	4.0	77
227	Significance of interfaces in solid-state cells with porous electrodes of mixed ionic–electronic conductors. Solid State Ionics, 1998, 107, 105-110.	1.3	76
228	Chemical, electrical, and thermal properties of strontium doped lanthanum vanadate. Solid State Ionics, 2005, 176, 1921-1928.	1.3	76
229	An Efficient SOFC Based on Samaria-Doped Ceria (SDC) Electrolyte. Journal of the Electrochemical Society, 2012, 159, B661-B665.	1.3	76
230	Li _{1.2} Ni _{0.13} Co _{0.13} Mn _{0.54} O ₂ with Controllable Morphology and Size for High Performance Lithium-Ion Batteries. ACS Applied Materials & Interfaces, 2017, 9, 25358-25368.	4.0	76
231	An effective strategy to enhancing tolerance to contaminants poisoning of solid oxide fuel cell cathodes. Nano Energy, 2018, 47, 474-480.	8.2	76
232	A self-healing layered GeP anode for high-performance Li-ion batteries enabled by low formation energy. Nano Energy, 2019, 61, 594-603.	8.2	76
233	Multifunctional Iron Oxide Nanoflake/Graphene Composites Derived from Mechanochemical Synthesis for Enhanced Lithium Storage and Electrocatalysis. ACS Applied Materials & Interfaces, 2015, 7, 14446-14455.	4.0	75
234	"Oneâ€forâ€All―Strategy in Fast Energy Storage: Production of Pillared MOF Nanorodâ€Templated Positive/Negative Electrodes for the Application of Highâ€Performance Hybrid Supercapacitor. Small, 2018, 14, e1800285.	5.2	75

#	Article	IF	CITATIONS
235	An effective method for enhancing oxygen evolution kinetics of LaMO3 (M = Ni, Co, Mn) perovskite catalysts and its application to a rechargeable zinc–air battery. Applied Catalysis B: Environmental, 2020, 262, 118291.	10.8	75
236	New insights into sulfur poisoning behavior of Ni-YSZ anode from long-term operation of anode-supported SOFCs. Energy and Environmental Science, 2010, 3, 1804.	15.6	74
237	Involvement of the VEGF receptor 3 in tubular morphogenesis demonstrated with a human anti-human VEGFR-3 monoclonal antibody that antagonizes receptor activation by VEGF-C. Journal of Cell Science, 2004, 117, 2745-2756.	1.2	73
238	Enhanced sinterability of BaZr0.1Ce0.7Y0.1Yb0.1O3â^î^by addition of nickel oxide. Journal of Power Sources, 2011, 196, 9980-9984.	4.0	73
239	Transport properties of LiMn2O4 electrode materials for lithium-ion batteries. Solid State Ionics, 1998, 110, 21-28.	1.3	72
240	Electrochemical insertion of lithium into multi-walled carbon nanotubes prepared by catalytic decomposition. Journal of Power Sources, 2002, 112, 216-221.	4.0	72
241	A honeycomb-like nitrogen-doped carbon as high-performance anode for potassium-ion batteries. Chemical Engineering Journal, 2020, 384, 123328.	6.6	72
242	Electrospun Porous Perovskite La _{0.6} Sr _{0.4} Co ₁ _– <i>_x</i> Fe <i>_x Nanofibers for Efficient Oxygen Evolution Reaction. Advanced Materials Interfaces, 2017, 4, 1700146.</i>	10 <sut< td=""><td>o>37⊄/sub><si< td=""></si<></td></sut<>	o>37⊄/sub> <si< td=""></si<>
243	Improving the Electrocatalytic Activity and Durability of the La _{0.6} Sr _{0.4} Co _{0.2} Fe _{0.8} O _{3â^î^} Cathode by Surface Modification. ACS Applied Materials & Interfaces, 2018, 10, 39785-39793.	4.0	71
244	MoS ₂ Decorated Fe ₃ O ₄ /Fe _{1–<i>x</i>} S@C Nanosheets as High-Performance Anode Materials for Lithium Ion and Sodium Ion Batteries. ACS Sustainable Chemistry and Engineering, 2017, 5, 4739-4745.	3.2	70
245	Integration of Zn–Ag and Zn–Air Batteries: A Hybrid Battery with the Advantages of Both. ACS Applied Materials & Interfaces, 2018, 10, 36873-36881.	4.0	70
246	Enhancing Li-S redox kinetics by fabrication of a three dimensional Co/CoP@nitrogen-doped carbon electrocatalyst. Chemical Engineering Journal, 2020, 380, 122595.	6.6	70
247	A high-performance electrode for supercapacitors: Silver nanoparticles grown on a porous perovskite-type material La0.7Sr0.3CoO3â~δ substrate. Chemical Engineering Journal, 2017, 328, 1-10.	6.6	69
248	A robust 2D organic polysulfane nanosheet with grafted polycyclic sulfur for highly reversible and durable lithium-organosulfur batteries. Nano Energy, 2019, 57, 635-643.	8.2	69
249	A Green Route to a Na ₂ FePO ₄ F-Based Cathode for Sodium Ion Batteries of High Rate and Long Cycling Life. ACS Applied Materials & Interfaces, 2017, 9, 16280-16287.	4.0	68
250	Advances in modeling and simulation of Li–air batteries. Progress in Energy and Combustion Science, 2017, 62, 155-189.	15.8	68
251	Lithiated zinc oxide nanorod arrays on copper current collectors for robust Li metal anodes. Chemical Engineering Journal, 2019, 378, 122243.	6.6	68
252	A mechanistic study of H2S decomposition on Ni- and Cu-based anode surfaces in a solid oxide fuel cell. Chemical Physics Letters, 2006, 421, 179-183.	1.2	67

#	Article	IF	CITATIONS
253	Surface regeneration of sulfur-poisoned Ni surfaces under SOFC operation conditions predicted by first-principles-based thermodynamic calculations. Journal of Power Sources, 2008, 176, 23-30.	4.0	67
254	3D hierarchically porous zinc–nickel–cobalt oxide nanosheets grown on Ni foam as binder-free electrodes for electrochemical energy storage. Journal of Materials Chemistry A, 2015, 3, 24022-24032.	5.2	67
255	A direct carbon solid oxide fuel cell operated on a plant derived biofuel with natural catalyst. Applied Energy, 2016, 179, 1232-1241.	5.1	67
256	Sb/C composite as a high-performance anode for sodium ion batteries. Electrochimica Acta, 2017, 242, 159-164.	2.6	67
257	Carbon fiber paper supported hybrid nanonet/nanoflower nickel oxide electrodes for high-performance pseudo-capacitors. Journal of Materials Chemistry A, 2013, 1, 7709.	5.2	66
258	Composite cathodes composed of NdBa _{0.5} Sr _{0.5} Co ₂ O _{5+δ} and Ce _{0.9} Gd _{0.1} O _{1.95} for intermediate-temperature solid oxidefuel cells. Journal of Materials Chemistry A, 2013, 1, 515-519.	5.2	66
259	Deactivation of nickel-based anode in solid oxide fuel cells operated on carbon-containing fuels. Journal of Power Sources, 2014, 268, 508-516.	4.0	66
260	An Efficient Bifunctional Air Electrode for Reversible Protonic Ceramic Electrochemical Cells. Advanced Functional Materials, 2021, 31, 2105386.	7.8	66
261	Phase transition–induced electrochemical performance enhancement of hierarchical CoCO3/CoO nanostructure for pseudocapacitor electrode. Nano Energy, 2015, 11, 736-745.	8.2	65
262	Design of high-performance cathode materials with single-phase pathway for sodium ion batteries: A study on P2-Nax(LiyMn1-y)O2 compounds. Journal of Power Sources, 2018, 381, 171-180.	4.0	65
263	Cation exchange synthesis of Ni _x Co _(3â^'x) O ₄ (<i>x</i> = 1.25) nanoparticles on aminated carbon nanotubes with high catalytic bifunctionality for the oxygen reduction/evolution reaction toward efficient Zn–air batteries. Journal of Materials Chemistry A, 2018, 6, 9517-9527.	5.2	65
264	Multi-functional anodes boost the transient power and durability of proton exchange membrane fuel cells. Nature Communications, 2020, 11, 1191.	5.8	65
265	Surface restructuring of a perovskite-type air electrode for reversible protonic ceramic electrochemical cells. Nature Communications, 2022, 13, 2207.	5.8	65
266	An efficient and durable anode for ammonia protonic ceramic fuel cells. Energy and Environmental Science, 2022, 15, 287-295.	15.6	64
267	X-ray photoelectron spectroscopy of La0.5Sr0.5MnO3. Materials Letters, 2005, 59, 1480-1483.	1.3	63
268	A First-Principles Analysis for Sulfur Tolerance of CeO ₂ in Solid Oxide Fuel Cells. Journal of Physical Chemistry C, 2007, 111, 11117-11122.	1.5	63
269	In situ X-ray diffraction investigation of CoSe2 anode for Na-ion storage: Effect of cut-off voltage on cycling stability. Electrochimica Acta, 2017, 258, 1387-1396.	2.6	63
270	A comparative investigation on direct carbon solid oxide fuel cells operated with fuels of biochar derived from wheat straw, corncob, and bagasse. Biomass and Bioenergy, 2019, 121, 56-63.	2.9	63

#	Article	IF	CITATIONS
271	Composite cathode based on yttria stabilized bismuth oxide for low-temperature solid oxide fuel cells. Applied Physics Letters, 2003, 82, 901-903.	1.5	62
272	A binder-free composite anode composed of CuO nanosheets and multi-wall carbon nanotubes for high-performance lithium-ion batteries. Electrochimica Acta, 2018, 267, 150-160.	2.6	62
273	Promotion of oxygen reduction reaction on a double perovskite electrode by a water-induced surface modification. Energy and Environmental Science, 2021, 14, 1506-1516.	15.6	62
274	Nanostructured LiMn2O4 prepared by a glycine-nitrate process for lithium-ion batteries. Solid State Ionics, 2004, 171, 25-31.	1.3	61
275	Preparation of dense and uniform La0.6Sr0.4Co0.2Fe0.8O3â^' (LSCF) films for fundamental studies of SOFC cathodes. Journal of Power Sources, 2009, 190, 307-310.	4.0	61
276	A more efficient anode microstructure for SOFCs based on proton conductors. International Journal of Hydrogen Energy, 2012, 37, 18342-18348.	3.8	61
277	A renewable natural cotton derived and nitrogen/sulfur co-doped carbon as a high-performance sodium ion battery anode. Materials Today Energy, 2018, 8, 37-44.	2.5	61
278	A hierarchical Ti2Nb10O29 composite electrode for high-power lithium-ion batteries and capacitors. Materials Today, 2021, 45, 8-19.	8.3	61
279	Functionally Graded Cathodes for Honeycomb Solid Oxide Fuel Cells. Electrochemical and Solid-State Letters, 2002, 5, A217.	2.2	60
280	A recombinant, fully human, bispecific antibody neutralizes the biological activities mediated by both vascular endothelial growth factor receptors 2 and 3. Molecular Cancer Therapeutics, 2005, 4, 427-434.	1.9	60
281	Intra- and Intermolecular Proton Transfer in 1H(2H)-1,2,3-Triazole Based Systems. Journal of Physical Chemistry A, 2006, 110, 2322-2324.	1.1	60
282	LSM-infiltrated LSCF cathodes for solid oxide fuel cells. Journal of Energy Chemistry, 2013, 22, 555-559.	7.1	59
283	SnS2 nanoparticles anchored on three-dimensional reduced graphene oxide as a durable anode for sodium ion batteries. Chemical Engineering Journal, 2018, 339, 78-84.	6.6	59
284	Fast Energy Storage in Two-Dimensional MoO ₂ Enabled by Uniform Oriented Tunnels. ACS Nano, 2019, 13, 9091-9099.	7.3	59
285	Synthesis and conductivity of proton-electrolyte membranes based on hybrid inorganic–organic copolymers. Electrochimica Acta, 2003, 48, 4271-4276.	2.6	58
286	High-performance anode-supported Solid Oxide Fuel Cells based on Ba(Zr0.1Ce0.7Y0.2)O3â^´î´ (BZCY) fabricated by a modified co-pressing process. Journal of Power Sources, 2010, 195, 1845-1848.	4.0	58
287	High-temperature surface enhanced Raman spectroscopy for in situ study of solid oxide fuel cell materials. Energy and Environmental Science, 2014, 7, 306-310.	15.6	58
288	Self-Templated Synthesis of Hierarchically Porous N-Doped Carbon Derived from Biomass for Supercapacitors. ACS Sustainable Chemistry and Engineering, 2018, 6, 13932-13939.	3.2	58

#	Article	IF	CITATIONS
289	Facile synthesis of M-Sb (M = Ni, Sn) alloy nanoparticles embedded in N-doped carbon nanosheets as high performance anode materials for lithium ion batteries. Chemical Engineering Journal, 2018, 348, 653-660.	6.6	58
290	Scalable synthesis of FeS ₂ nanoparticles encapsulated into N-doped carbon nanosheets as a high-performance sodium-ion battery anode. Nanoscale, 2019, 11, 3773-3779.	2.8	58
291	Enhanced Cr-tolerance of an SOFC cathode by an efficient electro-catalyst coating. Nano Energy, 2020, 72, 104704.	8.2	58
292	Investigating spiritual care perceptions and practice patterns in Hong Kong nurses: Results of a cluster analysis. Nurse Education Today, 2006, 26, 139-150.	1.4	57
293	Prediction of O2 Dissociation Kinetics on LaMnO3-Based Cathode Materials for Solid Oxide Fuel Cells. Journal of Physical Chemistry C, 2009, 113, 7290-7297.	1.5	57
294	Well-organized raspberry-like Ag@Cu bimetal nanoparticles for highly reliable and reproducible surface-enhanced Raman scattering. Nanoscale, 2013, 5, 11620.	2.8	57
295	The effect of composite organic acid (citric acid & tartaric acid) on microstructure and electrochemical properties of Li 1.2 Mn 0.54 Ni 0.13 Co 0.13 O 2 Li-rich layered oxides. Journal of Power Sources, 2017, 346, 31-39.	4.0	57
296	Melamine-assisted synthesis of Fe ₃ N featuring highly reversible crystalline-phase transformation for ultrastable sodium ion storage. Journal of Materials Chemistry A, 2020, 8, 6768-6775.	5.2	57
297	Highly Active and Durable Air Electrodes for Reversible Protonic Ceramic Electrochemical Cells Enabled by an Efficient Bifunctional Catalyst. Advanced Energy Materials, 2022, 12, .	10.2	57
298	Ab initio analysis of sulfur tolerance of Ni, Cu, and Ni–Cu alloys for solid oxide fuel cells. Journal of Alloys and Compounds, 2007, 427, 25-29.	2.8	56
299	Cu6Sn5@SnO2–C nanocomposite with stable core/shell structure as a high reversible anode for Li-ion batteries. Nano Energy, 2015, 18, 232-244.	8.2	56
300	Sulfonated Holey Graphene Oxide (SHGO) Filled Sulfonated Poly(ether ether ketone) Membrane: The Role of Holes in the SHGO in Improving Its Performance as Proton Exchange Membrane for Direct Methanol Fuel Cells. ACS Applied Materials & Interfaces, 2017, 9, 20046-20056.	4.0	56
301	Aluminum and Nitrogen Codoped Graphene: Highly Active and Durable Electrocatalyst for Oxygen Reduction Reaction. ACS Catalysis, 2019, 9, 610-619.	5.5	56
302	Enhancing Oxygen Reduction Activity and Cr Tolerance of Solid Oxide Fuel Cell Cathodes by a Multiphase Catalyst Coating. Advanced Functional Materials, 2021, 31, 2100034.	7.8	56
303	Flexible multiphysics simulation of porous electrodes: Conformal to 3D reconstructed microstructures. Nano Energy, 2013, 2, 105-115.	8.2	55
304	Exfoliated V 5 S 8 /graphite nanosheet with excellent electrochemical performance for enhanced lithium storage. Chemical Engineering Journal, 2017, 320, 485-493.	6.6	55
305	Co,N-codoped graphene as efficient electrocatalyst for hydrogen evolution reaction: Insight into the active centre. Journal of Power Sources, 2017, 363, 260-268.	4.0	55
306	Mn doped NaV3(PO4)3/C anode with high-rate and long cycle-life for sodium ion batteries. Energy Storage Materials, 2018, 12, 153-160.	9.5	55

#	Article	IF	CITATIONS
307	A new type of amperometric oxygen sensor based on a mixed-conducting composite membrane. Sensors and Actuators B: Chemical, 2001, 72, 35-40.	4.0	54
308	A Solid Oxide Fuel Cell Running on H[sub 2]Sâ^•CH[sub 4] Fuel Mixtures. Electrochemical and Solid-State Letters, 2006, 9, A31.	2.2	54
309	In Situ Probing of the Mechanisms of Coking Resistance on Catalyst-Modified Anodes for Solid Oxide Fuel Cells. Chemistry of Materials, 2015, 27, 822-828.	3.2	54
310	Inhibiting Sn coarsening to enhance the reversibility of conversion reaction in lithiated SnO2 anodes by application of super-elastic NiTi films. Acta Materialia, 2016, 109, 248-258.	3.8	54
311	Morphology and crystal phase evolution induced performance enhancement of MnO ₂ grown on reduced graphene oxide for lithium ion batteries. Journal of Materials Chemistry A, 2016, 4, 2643-2650.	5.2	54
312	Fluorine-Doped Carbon Surface Modification of Li-Rich Layered Oxide Composite Cathodes for High Performance Lithium-Ion Batteries. ACS Sustainable Chemistry and Engineering, 2018, 6, 16399-16411.	3.2	54
313	Enhanced Ionic/Electronic Transport in Nanoâ€īiO ₂ /Sheared CNT Composite Electrode for Na ⁺ Insertionâ€based Hybrid Ion apacitors. Advanced Functional Materials, 2020, 30, 1908309.	7.8	54
314	Fabrication of Sm0.5Sr0.5CoO3â^'δâ^'Sm0.1Ce0.9O2â^'δ cathodes for solid oxide fuel cells using combustion CVD. Solid State Ionics, 2004, 166, 261-268.	1.3	53
315	Synthesis and properties of phosphonic acid-grafted hybrid inorganic–organic polymer membranes. Journal of Materials Chemistry, 2006, 16, 858-864.	6.7	53
316	A new family of cation-disordered Zn(Cu)–Si–P compounds as high-performance anodes for next-generation Li-ion batteries. Energy and Environmental Science, 2019, 12, 2286-2297.	15.6	53
317	In-situ constructing Na3V2(PO4)2F3/carbon nanocubes for fast ion diffusion with high-performance Na+-storage. Chemical Engineering Journal, 2020, 387, 123952.	6.6	53
318	Electrochemical gas–electricity cogeneration through direct carbon solid oxide fuel cells. Journal of Power Sources, 2015, 277, 1-8.	4.0	52
319	Stability of Materials as Candidates for Sulfur-Resistant Anodes of Solid Oxide Fuel Cells. Journal of the Electrochemical Society, 2006, 153, A1302.	1.3	51
320	Tetrazoleâ€based, Anhydrous Proton Exchange Membranes for Fuel Cells. Advanced Materials, 2014, 26, 1277-1282.	11.1	51
321	Toward a new generation of low cost, efficient, and durable metal–air flow batteries. Journal of Materials Chemistry A, 2019, 7, 26744-26768.	5.2	51
322	In Situ Potential-Dependent FTIR Emission Spectroscopy. Journal of the Electrochemical Society, 2002, 149, A1293.	1.3	50
323	Preparation of Dense Platinum‥ttria Stabilized Zirconia and Yttria Stabilized Zirconia Films on Porous La _{0.9} Sr _{0.1} MnO ₃ (LSM) Substrates. Journal of the American Ceramic Society, 2001, 84, 283-88.	1.9	50
324	Electrical conductivity and electrochemical performance of cobalt-doped BaZr0.1Ce0.7Y0.2O3â~δ cathode. International Journal of Hydrogen Energy, 2011, 36, 2266-2270.	3.8	50

#	Article	IF	CITATIONS
325	Anode-supported micro-tubular SOFCs fabricated by a phase-inversion and dip-coating process. International Journal of Hydrogen Energy, 2011, 36, 5604-5610.	3.8	50
326	Atmospheric plasma-sprayed La _{0.8} Sr _{0.2} Ga _{0.8} Mg _{0.2} O ₃ electrolyte membranes for intermediate-temperature solid oxide fuel cells. Journal of Materials Chemistry A, 2015, 3, 7535-7553.	5.2	50
327	Electrochemical Oxidation of Carbon at High Temperature: Principles and Applications. Energy & Fuels, 2018, 32, 4107-4117.	2.5	50
328	A niobium oxide with a shear structure and planar defects for high-power lithium ion batteries. Energy and Environmental Science, 2022, 15, 254-264.	15.6	50
329	Stability of BaCe0.8Gd0.2 O 3 in a  H 2 O  ontaining Atmosphere at Intermediate the Electrochemical Society, 1997, 144, 2170-2175.	Temperatu 1.3	ures. Journal
330	Electrophoretic Deposition of YSZ Particles on Non-Conducting Porous NiO?YSZ Substrates for Solid Oxide Fuel Cell Applications. Journal of the American Ceramic Society, 2006, 89, 3003-3009.	1.9	49
331	The effect of platinum in a Nafion membrane on the durability of the membrane under fuel cell conditions. Journal of Power Sources, 2010, 195, 4606-4612.	4.0	49
332	Surfactants assisted synthesis and electrochemical properties of nano-LiFePO 4 /C cathode materials for low temperature applications. Journal of Power Sources, 2015, 288, 337-344.	4.0	49
333	Preparation of mesoporous SnO2–SiO2 composite as electrodes for lithium batteries. Chemical Communications, 2000, , 2095-2096.	2.2	48
334	High-performance Ni–BaZr0.1Ce0.7Y0.1Yb0.1O3â~'î́ (BZCYYb) membranes for hydrogen separation. International Journal of Hydrogen Energy, 2013, 38, 14743-14749.	3.8	48
335	Perovskite SrCo _{0.9} Nb _{0.1} O _{3â^'<i>δ</i>} as an Anionâ€Intercalated Electrode Material for Supercapacitors with Ultrahigh Volumetric Energy Density. Angewandte Chemie, 2016, 128, 9728-9731.	1.6	48
336	High-Performance Electrodes for a Hybrid Supercapacitor Derived from a Metal–Organic Framework/Graphene Composite. ACS Applied Energy Materials, 2019, 2, 5029-5038.	2.5	48
337	Metal–Organic Frameworksâ€Derived Nitrogenâ€Doped Porous Carbon Nanocubes with Embedded Co Nanoparticles as Efficient Sulfur Immobilizers for Room Temperature Sodium–Sulfur Batteries. Small Methods, 2021, 5, e2100455.	4.6	48
338	Interfacial resistances of Ni–BCY mixed-conducting membranes for hydrogen separation. Solid State Ionics, 2003, 159, 121-134.	1.3	47
339	A Sulfur-Tolerant Anode Material for SOFCs. Electrochemical and Solid-State Letters, 2005, 8, A406.	2.2	47
340	An Efficient Steamâ€Induced Heterostructured Air Electrode for Protonic Ceramic Electrochemical Cells. Advanced Functional Materials, 2022, 32, .	7.8	47
341	Distributions of Charged Defects in Mixed Ionicâ€Electronic Conductors: I. General Equations for Homogeneous Mixed Ionicâ€Electronic Conductors. Journal of the Electrochemical Society, 1997, 144, 1813-1834.	1.3	46
342	Sulfur-Tolerant Materials for the Hydrogen Sulfide SOFC. Electrochemical and Solid-State Letters, 2004, 7, A324.	2.2	46

#	Article	IF	CITATIONS
343	Preparation of NiO-YSZ/YSZ bi-layers for solid oxide fuel cells by electrophoretic deposition. Journal of Power Sources, 2006, 160, 207-214.	4.0	46

A Durable Alternative for Protonâ \in Exchange Membranes: Sulfonated Poly(Benzoxazole Thioether) Tj ETQq0 0 0 rgBT/Qverlock 10 Tf 50 46

345	Deformable fibrous carbon supported ultrafine nano-SnO ₂ as a high volumetric capacity and cyclic durable anode for Li storage. Journal of Materials Chemistry A, 2015, 3, 15097-15107.	5.2	46
346	A high-performance oxygen electrode for Li–O ₂ batteries: Mo ₂ C nanoparticles grown on carbon fibers. Journal of Materials Chemistry A, 2017, 5, 5690-5695.	5.2	46
347	A high performance direct carbon solid oxide fuel cell fueled by Ca-loaded activated carbon. International Journal of Hydrogen Energy, 2017, 42, 21167-21176.	3.8	46
348	Electronic coupling induced high performance of N, S-codoped graphene supported CoS2 nanoparticles for catalytic reduction and evolution of oxygen. Journal of Power Sources, 2018, 389, 178-187.	4.0	46
349	Uniform Li deposition regulated <i>via</i> three-dimensional polyvinyl alcohol nanofiber networks for effective Li metal anodes. Nanoscale, 2018, 10, 10018-10024.	2.8	46
350	Direct synthesis of FeS/N-doped carbon composite for high-performance sodium-ion batteries. Journal of Materials Chemistry A, 2018, 6, 24702-24708.	5.2	46
351	Amine group induced high activity of highly torn amine functionalized nitrogen-doped graphene as the metal-free catalyst for hydrogen evolution reaction. Carbon, 2018, 138, 169-178.	5.4	46
352	Fundamental issues in modeling of mixed ionic-electronic conductors (MIECs). Solid State Ionics, 1999, 118, 11-21.	1.3	45
353	Distributions of noble metal Pd and Pt in mesoporous silica. Applied Physics Letters, 2002, 81, 3449-3451.	1.5	45
354	Pre-reforming of propane for low-temperature SOFCs. Solid State Ionics, 2004, 166, 269-273.	1.3	45
355	Nanocomposite Electrodes Fabricated by a Particle-Solution Spraying Process for Low-Temperature SOFCs. Chemistry of Materials, 2004, 16, 3502-3506.	3.2	45
356	Microstructure and electrochemical properties of cathode materials for SOFCs prepared via pulsed laser deposition. Journal of Power Sources, 2006, 161, 250-255.	4.0	45
357	Surface Modification of Ni-YSZ Using Niobium Oxide for Sulfur-Tolerant Anodes in Solid Oxide Fuel Cells. Journal of the Electrochemical Society, 2008, 155, B449.	1.3	45
358	Direct operation of Ag-based anode solid oxide fuel cells on propane. Journal of Power Sources, 2017, 366, 56-64.	4.0	45
359	A novel NiCo2O4@GO hybrid composite with core-shell structure as high-performance anodes for lithium-ion batteries. Journal of Alloys and Compounds, 2018, 731, 1095-1102.	2.8	45
360	Ultra-thick electrodes based on activated wood-carbon towards high-performance quasi-solid-state supercapacitors. Physical Chemistry Chemical Physics, 2020, 22, 2073-2080.	1.3	45

#	Article	IF	CITATIONS
361	Hierarchical porous carbon sheets for high-performance room temperature sodium–sulfur batteries: integration of nitrogen-self-doping and space confinement. Journal of Materials Chemistry A, 2020, 8, 24590-24597.	5.2	45
362	Flexible nonwoven ZrO2 ceramic membrane as an electrochemically stable and flame-resistant separator for high-power rechargeable batteries. Chemical Engineering Journal, 2020, 388, 124259.	6.6	45
363	Engineering the architecture and oxygen deficiency of T-Nb2O5-carbon-graphene composite for high-rate lithium-ion batteries. Nano Energy, 2021, 89, 106398.	8.2	45
364	Electricity generation from corn cob char though a direct carbon solid oxide fuel cell. Biomass and Bioenergy, 2016, 91, 250-258.	2.9	44
365	Study of transition metal oxide doped LaGaO 3 as electrode materials for LSGM-based solid oxide fuel cells. Journal of Solid State Electrochemistry, 1998, 3, 7-14.	1.2	43
366	LSM-GDC Composite Cathodes Derived from a Sol-Gel Process. Electrochemical and Solid-State Letters, 2003, 6, A290.	2.2	43
367	All-solid-state direct carbon fuel cells with thin yttrium-stabilized-zirconia electrolyte supported on nickel and iron bimetal-based anodes. International Journal of Hydrogen Energy, 2016, 41, 9048-9058.	3.8	43
368	Recent Advances in Titanium Niobium Oxide Anodes for High-Power Lithium-Ion Batteries. Energy & Fuels, 2020, 34, 13321-13334.	2.5	43
369	Microwave Combustion for Modification of Transition Metal Oxides. Advanced Functional Materials, 2016, 26, 7263-7270.	7.8	42
370	Sb@C/expanded graphite as high-performance anode material for lithium ion batteries. Journal of Alloys and Compounds, 2018, 744, 481-486.	2.8	42
371	Enhancing sinterability and electrochemical properties of Ba(Zr0.1Ce0.7Y0.2)O3-δ proton conducting electrolyte for solid oxide fuel cells byÂaddition of NiO. International Journal of Hydrogen Energy, 2018, 43, 13501-13511.	3.8	42
372	Effective Promotion of Oxygen Reduction Reaction by in Situ Formation of Nanostructured Catalyst. ACS Catalysis, 2019, 9, 7137-7142.	5.5	42
373	A Scalable Approach for Dendrite-Free Alkali Metal Anodes via Room-Temperature Facile Surface Fluorination. ACS Applied Materials & Interfaces, 2019, 11, 4962-4968.	4.0	42
374	High-performance, ceria-based solid oxide fuel cells fabricated at low temperatures. Journal of Power Sources, 2013, 241, 454-459.	4.0	41
375	Chemiluminescence Energy Transfer Reaction for the On-Line Preparation of Peroxymonocarbonate and Eu(II)â^'Dipicolinate Complex. Journal of Physical Chemistry A, 2006, 110, 7509-7514.	1.1	40
376	Effects of pore formers on microstructure and performance of cathode membranes for solid oxide fuel cells. Journal of Power Sources, 2011, 196, 9975-9979.	4.0	40
377	Behavior of strontium- and magnesium-doped gallate electrolyte in direct carbon solid oxide fuel cells. Journal of Alloys and Compounds, 2014, 608, 272-277.	2.8	40
378	Effects of doping alumina on the electrical and sintering performances of yttrium-stabilized-zirconia. Solid State Ionics, 2016, 289, 28-34.	1.3	40

#	Article	IF	CITATIONS
379	Porous Functionalized Self-Standing Carbon Fiber Paper Electrodes for High-Performance Capacitive Energy Storage. ACS Applied Materials & Interfaces, 2017, 9, 13173-13180.	4.0	40
380	Efficient CO2 Utilization via a Hybrid Na-CO2 System Based on CO2 Dissolution. IScience, 2018, 9, 278-285.	1.9	40
381	Electrochemical Properties of Li-Zn Alloy Electrodes Prepared by Kinetically Controlled Vapor Deposition for Lithium Batteries. Electrochemical and Solid-State Letters, 1999, 3, 312.	2.2	39
382	Synthesis and properties of imidazole-grafted hybrid inorganic–organic polymer membranes. Electrochimica Acta, 2006, 51, 1351-1358.	2.6	39
383	Impacts of climatic and atmospheric changes on carbon dynamics in the Great Smoky Mountains National Park. Environmental Pollution, 2007, 149, 336-347.	3.7	39
384	Anode-supported tubular SOFCs based on BaZr0.1Ce0.7Y0.1Yb0.1O3â^îr´electrolyte fabricated by dip coating. Electrochemistry Communications, 2011, 13, 615-618.	2.3	39
385	A direct flame solid oxide fuel cell for potential combined heat and power generation. International Journal of Hydrogen Energy, 2012, 37, 8621-8629.	3.8	39
386	High performance solid oxide electrolysis cells using Pr0.8Sr1.2(Co,Fe)0.8Nb0.2O4+Î′–Co–Fe alloy hydrogen electrodes. International Journal of Hydrogen Energy, 2013, 38, 11202-11208.	3.8	39
387	Snâ€MoS ₂ @C Microspheres as a Sodiumâ€lon Battery Anode Material with High Capacity and Long Cycle Life. Chemistry - A European Journal, 2017, 23, 5051-5058.	1.7	39
388	Enhanced overall water electrolysis on a bifunctional perovskite oxide through interfacial engineering. Electrochimica Acta, 2019, 318, 120-129.	2.6	39
389	P3-type K0.5Mn0.72Ni0.15Co0.13O2 microspheres as cathode materials for high performance potassium-ion batteries. Chemical Engineering Journal, 2020, 392, 123735.	6.6	39
390	Characteristic Thickness for a Dense La[sub 0.8]Sr[sub 0.2]MnO[sub 3] Electrode. Electrochemical and Solid-State Letters, 2005, 8, A592.	2.2	38
391	Singlet oxygen generated from the decomposition of peroxymonocarbonate and its observation with chemiluminescence method. Spectrochimica Acta - Part A: Molecular and Biomolecular Spectroscopy, 2009, 72, 126-132.	2.0	38
392	Application of surface enhanced Raman spectroscopy to the study of SOFC electrode surfaces. Physical Chemistry Chemical Physics, 2012, 14, 5919.	1.3	38
393	Hydrothermal synthesis of LiMn2O4 onto carbon fiber paper current collector for binder free lithium-ion battery positive electrodes. Journal of Power Sources, 2014, 251, 411-416.	4.0	38
394	Facile Strategy to Low-Cost Synthesis of Hierarchically Porous, Active Carbon of High Graphitization for Energy Storage. ACS Applied Materials & amp; Interfaces, 2018, 10, 21573-21581.	4.0	38
395	A direct carbon solid oxide fuel cell fueled with char from wheat straw. International Journal of Energy Research, 2019, 43, 2468-2477.	2.2	38
396	Porous Ultrathin W-Doped VO ₂ Nanosheets Enable Boosted Zn ²⁺ (De)Intercalation Kinetics in VO ₂ for High-Performance Aqueous Zn-Ion Batteries. ACS Sustainable Chemistry and Engineering, 2021, 9, 14193-14201.	3.2	38

#	Article	IF	CITATIONS
397	A Singleâ€Atom Feâ€N Catalyst with Ultrahigh Utilization of Active Sites for Efficient Oxygen Reduction. Small, 2022, 18, .	5.2	38
398	Hydrogen Permeation and Chemical Stability of Cermet [Ni–Ba(Zr[sub 0.8â^'x]Ce[sub x]Y[sub 0.2])O[sub 3]] Membranes. Electrochemical and Solid-State Letters, 2005, 8, J35.	2.2	37
399	Fabrication and characterization of functionally-graded LSCF cathodes by tape casting. International Journal of Hydrogen Energy, 2013, 38, 1082-1087.	3.8	37
400	A Highly Ordered Hydrophilic–Hydrophobic Janus Biâ€Functional Layer with Ultralow Pt Loading and Fast Gas/Water Transport for Fuel Cells. Energy and Environmental Materials, 2021, 4, 126-133.	7.3	37
401	Phase Engineering of Atomically Thin Perovskite Oxide for Highly Active Oxygen Evolution. Advanced Functional Materials, 2021, 31, 2102002.	7.8	37
402	A highly efficient and durable air electrode for intermediate-temperature reversible solid oxide cells. Applied Catalysis B: Environmental, 2021, 299, 120631.	10.8	37
403	Classical, phenomenological analysis of the kinetics of reactions at the gas-exposed surface of mixed ionic electronic conductors. Journal of Solid State Electrochemistry, 2006, 10, 575-580.	1.2	36
404	Monitoring Agâ^'Cr Interactions in SOFC Cathodes Using Raman Spectroscopy. Journal of Physical Chemistry C, 2008, 112, 13299-13303.	1.5	36
405	A mixed-conducting BaPr0.8In0.2O3â [~] δ cathode for proton-conducting solid oxide fuel cells. Electrochemistry Communications, 2013, 27, 19-21.	2.3	36
406	Hierarchical Design of Mn ₂ P Nanoparticles Embedded in N,P-Codoped Porous Carbon Nanosheets Enables Highly Durable Lithium Storage. ACS Applied Materials & Interfaces, 2020, 12, 36247-36258.	4.0	36
407	Development of a selective gas sensor utilizing a perm-selective zeolite membrane. Journal of Materials Science, 2003, 38, 4307-4317.	1.7	35
408	A triazole-based polymer electrolyte membrane for fuel cells operated in a wide temperature range (25–150°C) with little humidification. Journal of Power Sources, 2013, 241, 219-224.	4.0	35
409	Grapheneâ€Encapsulated Nanosheetâ€Assembled Zinc–Nickel–Cobalt Oxide Microspheres for Enhanced Lithium Storage. ChemSusChem, 2016, 9, 186-196.	3.6	35
410	Nanoporous NiO/Ni(OH) ₂ Plates Incorporated with Carbon Nanotubes as Active Materials of Rechargeable Hybrid Zinc Batteries for Improved Energy Efficiency and High-Rate Capability. Journal of the Electrochemical Society, 2018, 165, A2119-A2126.	1.3	35
411	A promising water-in-salt electrolyte for aqueous based electrochemical energy storage cells with a wide potential window: highly concentrated HCOOK. Chemical Communications, 2019, 55, 12817-12820.	2.2	35
412	Partially Reduced Titanium Niobium Oxide: A Highâ€Performance Lithiumâ€Storage Material in a Broad Temperature Range. Advanced Science, 2022, 9, e2105119.	5.6	35
413	Materials considerations for application to solid-state electrochemical devices. Solid State Ionics, 1992, 52, 57-68.	1.3	34
414	An operando surface enhanced Raman spectroscopy (SERS) study of carbon deposition on SOFC anodes. Physical Chemistry Chemical Physics, 2015, 17, 21112-21119.	1.3	34

#	Article	IF	CITATIONS
415	An investigation on the kinetics of direct carbon solid oxide fuel cells. Journal of Solid State Electrochemistry, 2016, 20, 2207-2216.	1.2	34
416	The Structure of Oxygen Vacancies in the Near-Surface of Reduced CeO2 (111) Under Strain. Frontiers in Chemistry, 2019, 7, 436.	1.8	34
417	Electrocatalytic properties of La 0.9 Sr 0.1 MnO 3 -based electrodes for oxygen reduction. Journal of Solid State Electrochemistry, 2002, 6, 384-390.	1.2	33
418	Three-Dimensional Microstructural Imaging of Sulfur Poisoning-Induced Degradation in a Ni-YSZ Anode of Solid Oxide Fuel Cells. Scientific Reports, 2014, 4, 5246.	1.6	33
419	Rationally Designed 3D Fe and N Codoped Graphene with Superior Electrocatalytic Activity toward Oxygen Reduction. Small, 2016, 12, 2549-2553.	5.2	33
420	Highly Efficient CO ₂ Utilization via Aqueous Zinc– or Aluminum–CO ₂ Systems for Hydrogen Gas Evolution and Electricity Production. Angewandte Chemie - International Edition, 2019, 58, 9506-9511.	7.2	33
421	Structural design of Ge-based anodes with chemical bonding for high-performance Na-ion batteries. Energy Storage Materials, 2019, 20, 380-387.	9.5	33
422	Electrosynthesis of Ammonia Using Porous Bimetallic Pd–Ag Nanocatalysts in Liquid- and Gas-Phase Systems. ACS Catalysis, 2020, 10, 10197-10206.	5.5	33
423	Yolk-shell structured CuSi2P3@Graphene nanocomposite anode for long-life and high-rate lithium-ion batteries. Nano Energy, 2021, 80, 105506.	8.2	33
424	A high-performance and durable direct NH3 tubular protonic ceramic fuel cell integrated with an internal catalyst layer. Applied Catalysis B: Environmental, 2022, 306, 121071.	10.8	33
425	Preparation and electrochemical properties of glass-polymer composite electrolytes for lithium batteries. Electrochimica Acta, 1997, 42, 1481-1488.	2.6	32
426	Mixed Tocopherols Have a Stronger Inhibitory Effect on Lipid Peroxidation Than α-Tocopherol Alone. Journal of Cardiovascular Pharmacology, 2002, 39, 714-721.	0.8	32
427	A high-performance intermediate-to-low temperature protonic ceramic fuel cell with in-situ exsolved nickel nanoparticles in the anode. Ceramics International, 2020, 46, 19952-19959.	2.3	32
428	Nanoscale surface modification of P2-type Na0.65[Mn0.70Ni0.16Co0.14]O2 cathode material for high-performance sodium-ion batteries. Chemical Engineering Journal, 2021, 404, 126446.	6.6	32
429	Refinement of the bulk defect model for LaxSr1â~'xMnO3±δâ~†. Solid State Ionics, 2008, 178, 1950-1957.	1.3	31
430	Impact of Strain-Induced Changes in Defect Chemistry on Catalytic Activity of Nd ₂ NiO _{4+1´} Electrodes. ACS Applied Materials & Interfaces, 2018, 10, 36926-36932.	4.0	31
431	Multiple Effects of Iron and Nickel Additives on the Properties of Proton Conducting Yttrium-Doped Barium Cerate-Zirconate Electrolytes for High-Performance Solid Oxide Fuel Cells. ACS Applied Materials & Interfaces, 2020, 12, 50433-50445.	4.0	31
432	Recent Advances and Prospects of Atomic Substitution on Layered Positive Materials for Lithiumâ€ion Battery. Advanced Energy Materials, 2021, 11, 2003197.	10.2	31

#	Article	IF	CITATIONS
433	Luminescence properties of Mn2+ doped Zn2SiO4 phosphor films synthesized by combustion CVD. Journal of Luminescence, 2006, 121, 595-600.	1.5	30
434	Continuum and Quantum-Chemical Modeling of Oxygen Reduction on the Cathode in a Solid Oxide Fuel Cell. Topics in Catalysis, 2007, 46, 386-401.	1.3	30
435	Operando and Inâ€situ Xâ€ray Spectroscopies of Degradation in La _{0.6} Sr _{0.4} Co _{0.2} Fe _{0.8} O _{3â^'<i>δ</i>} Thin Film Cathodes in Fuel Cells. ChemSusChem, 2014, 7, 3078-3087.	3.6	30
436	A high-performance, cobalt-free cathode for intermediate-temperature solid oxide fuel cells with excellent CO2 tolerance. Journal of Power Sources, 2016, 319, 178-184.	4.0	30
437	Segregation Induced Selfâ€Assembly of Highly Active Perovskite for Rapid Oxygen Reduction Reaction. Advanced Energy Materials, 2018, 8, 1801893.	10.2	30
438	In Situ and Surface-Enhanced Raman Spectroscopy Study of Electrode Materials in Solid Oxide Fuel Cells. Electrochemical Energy Reviews, 2018, 1, 433-459.	13.1	30
439	An amorphous Zn–P/graphite composite with chemical bonding for ultra-reversible lithium storage. Journal of Materials Chemistry A, 2019, 7, 16785-16792.	5.2	30
440	Plastic waste fuelled solid oxide fuel cell system for power and carbon nanotube cogeneration. International Journal of Hydrogen Energy, 2019, 44, 1867-1876.	3.8	30
441	Ambient Ammonia Electrosynthesis from Nitrogen and Water by Incorporating Palladium in Bimetallic Gold–Silver Nanocages. Journal of the Electrochemical Society, 2020, 167, 054511.	1.3	30
442	In Situ Exsolution of Coreâ€Shell Structured NiFe/FeO _x Nanoparticles on Pr _{0.4} Sr _{1.6} (NiFe) _{1.5} Mo _{0.5} O _{6â€Î} for CO ₂ Electrolysis. Advanced Functional Materials, 2022, 32, .	7.8	30
443	Preparation and Characterization of (<scp>La_{0.8}Sr_{0.2})_{0.95}MnO_{3â[^]î}</scp> (<scp>LSM</scp>) Thin Films and <scp>LSM/LSCF</scp> Interface for Solid Oxide Fuel Cells. Journal of the American Ceramic Society. 2011, 94, 3340-3345.	1.9	29
444	Enhancing Sulfur Tolerance of a Ni-YSZ Anode through BaZr _{0.1} Ce _{0.7} Y _{0.1} Yb _{0.1} O _{3â^'<i>δ</i>} Infiltration Journal of the Electrochemical Society, 2014, 161, F668-F673.	1.1.3	29
445	Silver―BaCe0.8Gd0.2 O 3 Composites as Cathode Materials for SOFCs Using BaCeO3â€Based Electroly Journal of the Electrochemical Society, 1996, 143, 859-864.	yteş. 1.3	28
446	Structural and Electrical Characterization of a Novel Mixed Conductor: CeO[sub 2]-Sm[sub 2]O[sub 3]-ZrO[sub 2] Solid Solution. Journal of the Electrochemical Society, 2000, 147, 4196.	1.3	28
447	A photolithographic process for investigation of electrode reaction sites in solid oxide fuel cells. Solid State Ionics, 2005, 176, 1-8.	1.3	28
448	High-performance solid oxide fuel cells based on a thin La0.8Sr0.2Ga0.8Mg0.2O3â^î^ electrolyte membrane supported by a nickel-based anode of unique architecture. Journal of Power Sources, 2016, 301, 199-203.	4.0	28
449	A family of MOFs@Wood-Derived hierarchical porous composites as freestanding thick electrodes of solid supercapacitors with enhanced areal capacitances and energy densities. Materials Today Energy, 2022, 24, 100951.	2.5	28
450	Electrical properties, thermodynamic behavior, and defect analysis of Lan+1NinO3n+1+δ infiltrated into YSZ scaffolds as cathodes for intermediate-temperature SOFCs. RSC Advances, 2012, 2, 4648.	1.7	27

#	Article	IF	CITATIONS
451	Impedance Spectroscopy Study of an SDC-based SOFC with High Open Circuit Voltage. Electrochimica Acta, 2015, 177, 227-236.	2.6	27
452	Electrokinetic Proton Transport in Triple (H ⁺ /O ^{2â^'} /e ^{â^'}) Conducting Oxides as a Key Descriptor for Highly Efficient Protonic Ceramic Fuel Cells. Advanced Science, 2021, 8, e2004099.	5.6	27
453	Polyorganodisulfide electrodes for solid-state batteries and electrochromic devices. Solid State Ionics, 1993, 60, 175-187.	1.3	26
454	A Two-Dimensional Model and Numerical Treatment for Mixed Conducting Thin Films. Journal of the Electrochemical Society, 2007, 154, A421.	1.3	26
455	Fabrication of 3-Dimensional Porous Graphene Materials for Lithium Ion Batteries. Electrochimica Acta, 2014, 146, 437-446.	2.6	26
456	Exploration of VPO ₄ as a new anode material for sodium-ion batteries. Chemical Communications, 2017, 53, 12696-12699.	2.2	26
457	Electrochemical Properties of BaCe0.8Gd0.2 O 3 Electrolyte Films Deposited on Ni â€â€‰BaCe0.8 Substrates. Journal of the Electrochemical Society, 1997, 144, 1035-1040.	8Gd0.2â€% 1.3	‰Qậ€‰3
458	Interfacial Polarization Characteristics of Pt   BaCe0.8Gd0.2 O 3   Pt Cells at Interm Journal of the Electrochemical Society, 1997, 144, 3561-3567.	ediate Ten 1.3	nperatures.
459	Thermally sprayed high-performance porous metal-supported solid oxide fuel cells with nanostructured La _{0.6} Sr _{0.4} Co _{0.2} Fe _{0.8} O _{3â~î~} cathodes. Journal of Materials Chemistry A. 2016, 4. 7461-7468.	5.2	25
460	Promising Proton Conductor for Intermediate-Temperature Fuel Cells: Li _{13.9} Sr _{0.1} Zn(GeO ₄) ₄ . Chemistry of Materials, 2017, 29, 1490-1495.	3.2	25
461	Single Cobalt Atoms Decorated Nâ€doped Carbon Polyhedron Enabled Dendriteâ€Free Sodium Metal Anode. Small Methods, 2021, 5, e2100833.	4.6	25
462	Stabilities and electrical conductivities of electrode materials for use in H2S-containing gases. Journal of Solid State Electrochemistry, 2001, 5, 188-195.	1.2	24
463	Surface states in template synthesized tin oxide nanoparticles. Journal of Applied Physics, 2004, 95, 2178-2180.	1.1	24
464	New insights into carbon deposition mechanism of nickel/yttrium-stabilized zirconia cermet from methane by in situ investigation. Applied Energy, 2019, 256, 113910.	5.1	24
465	An improved oxygen reduction reaction activity and CO2-tolerance of La0.6Sr0.4Co0.2Fe0.8O3-δ achieved by a surface modification with barium cobaltite coatings. Journal of Power Sources, 2021, 514, 230573.	4.0	24
466	Surface Regulating of a Doubleâ€Perovskite Electrode for Protonic Ceramic Fuel Cells to Enhance Oxygen Reduction Activity and Contaminants Poisoning Tolerance. Advanced Energy Materials, 2022, 12, .	10.2	24
467	Triple-Phase Boundary and Surface Transport in Mixed Conducting Patterned Electrodes. Journal of the Electrochemical Society, 2008, 155, B635.	1.3	23
468	Quantitative nanoscale tracking of oxygen vacancy diffusion inside single ceria grains by in situ transmission electron microscopy. Materials Today, 2020, 38, 24-34.	8.3	23

#	Article	IF	CITATIONS
469	A straight, open and macro-porous fuel electrode-supported protonic ceramic electrochemical cell. Journal of Materials Chemistry A, 2021, 9, 10789-10795.	5.2	23
470	Lithium insertion into chemically etched multi-walled carbon nanotubes. Journal of Solid State Electrochemistry, 2004, 8, 908-913.	1.2	22
471	A stochastic geometry based model for total triple phase boundary length in composite cathodes for solid oxide fuel cells. Journal of Power Sources, 2009, 194, 303-312.	4.0	22
472	Reverse micelles template assisted fabrication of ZnO hollow nanospheres and hexagonal microtubes by a novel fast microemulsion-based hydrothermal method. Journal of Sol-Gel Science and Technology, 2010, 53, 101-106.	1.1	22
473	Investigation of sheet resistance in thin-film mixed-conducting solid oxide fuel cell cathode test cells. Journal of Power Sources, 2010, 195, 5155-5166.	4.0	22
474	Electrical and electrocatalytic properties of a La0.8Sr0.2Co0.17Mn0.83O3â~δ cathode for intermediate-temperature solid oxide fuel cells. Journal of Power Sources, 2012, 205, 80-85.	4.0	22
475	Intermediate temperature micro-tubular SOFCs with enhanced performance and thermal stability. Electrochemistry Communications, 2013, 34, 231-234.	2.3	22
476	Investigation into the energy storage behaviour of layered α-V2O5 as a pseudo-capacitive electrode using operando Raman spectroscopy and a quartz crystal microbalance. Physical Chemistry Chemical Physics, 2017, 19, 24689-24695.	1.3	22
477	High-Performance Quasi-Solid-State Supercapacitor Based on CuO Nanoparticles with Commercial-Level Mass Loading on Ceramic Material La _{1-<i>x</i>} Sr _{<i>x</i>} CoO _{3-î´} as Cathode. ACS Applied Energy Materials. 2019. 2. 1480-1488.	2.5	22
478	Investigation of the mechanism of sol-gel formation in the Sr(NO ₃) ₂ /citric acid/ethylene glycol system by solution state ⁸⁷ Sr nuclear magnetic resonance spectroscopy. Journal of Materials Research, 2000, 15, 2393-2399.	1.2	21
479	Flow-Injection Chemiluminescence Determination of Formaldehyde with a Bromate-Rhodamine 6G System. Analytical Sciences, 2003, 19, 1643-1646.	0.8	21
480	Synthesis of Tin Oxide Nanostructures with Controlled Particle Size Using Mesoporous Frameworks. Electrochemical and Solid-State Letters, 2004, 7, G93.	2.2	21
481	In vitro monitoring of nanogram levels of naproxen in human urine using flow injection chemiluminescence. Analytica Chimica Acta, 2006, 558, 296-301.	2.6	21
482	Strong coupling between Rhodamine 6G and localized surface plasmon resonance of immobile Ag nanoclusters fabricated by direct current sputtering. Applied Physics Letters, 2013, 102, .	1.5	21
483	A novel low-pressure injection molding technique for fabricating anode supported solid oxide fuel cells. International Journal of Hydrogen Energy, 2014, 39, 5105-5112.	3.8	21
484	Investigation of A-site deficient Ba0.9Co0.7Fe0.2Nb0.1O3â^îî′ cathode for proton conducting electrolyte based solid oxide fuel cells. International Journal of Hydrogen Energy, 2014, 39, 8431-8436.	3.8	21
485	Revealing the effects of oxygen defects on the electro-catalytic activity of nickel oxide. International Journal of Hydrogen Energy, 2020, 45, 424-432.	3.8	21
486	Organic polysulfanes grafted on porous graphene as an electrode for high-performance lithium organosulfur batteries. Journal of Power Sources, 2021, 491, 229617.	4.0	21

#	Article	IF	CITATIONS
487	Colloidal Processing of BaCeO3â€Based Electrolyte Films. Journal of the Electrochemical Society, 1996, 143, 3239-3244.	1.3	20
488	Characterization of a fission yeast subunit of an RNA polymerase I essential transcription initiation factor, SpRrn7h/TAF I 68, that bridges yeast and mammals: association with SpRrn11h and the core ribosomal RNA gene promoter. Gene, 2002, 291, 187-201.	1.0	20
489	Agâ€Bi _{1.5} Y _{0.5} O ₃ Composite Cathode Materials for BaCe _{0.8} Gd _{0.2} O ₃ â€Based Solid Oxide Fuel Cells. Journal of the American Ceramic Society, 1998, 81, 1215-1220.	1.9	20
490	On-line preparation of peroxymonocarbonate and its application for the study of energy transfer chemiluminescence to lanthanide inorganic coordinate complexes. Luminescence, 2006, 21, 179-185.	1.5	20
491	High-Performance, Thermal Cycling Stable, Coking-Tolerant Solid Oxide Fuel Cells with Nanostructured Electrodes. ACS Applied Materials & Interfaces, 2021, 13, 4993-4999.	4.0	20
492	Critical role of acceptor dopants in designing highly stable and compatible proton-conducting electrolytes for reversible solid oxide cells. Energy and Environmental Science, 2022, 15, 2992-3003.	15.6	20
493	Flow injection chemiluminescence determination of l-cysteine in amino acid mixture and human urine with the BrO3??quinine system. Analytical and Bioanalytical Chemistry, 2003, 377, 1212-1216.	1.9	19
494	Signatures of epitaxial graphene grown on Si-terminated 6H-SiC (0001). Surface Science, 2010, 604, 84-88.	0.8	19
495	High surface area, micro/mesoporous carbon particles with selectable 3-D biogenic morphologies for tailored catalysis, filtration, or adsorption. Energy and Environmental Science, 2011, 4, 3980.	15.6	19
496	Atmospheric plasma-sprayed BaZr0.1Ce0.7Y0.1Yb0.1O3â^´î´ (BZCYYb) electrolyte membranes for intermediate-temperature solid oxide fuel cells. Ceramics International, 2016, 42, 19231-19236.	2.3	19
497	3D-Hierarchical porous nickel sculptured by a simple redox process and its application in high-performance supercapacitors. Journal of Materials Chemistry A, 2017, 5, 20709-20719.	5.2	19
498	Hierarchically Porous Co and N odoped Carbon Hollow Structure Derived from PS@ZIFâ€67 as an Electrocatalyst for Oxygen Reduction. ChemistrySelect, 2018, 3, 4831-4837.	0.7	19
499	Effect of counter diffusion of CO and CO2 between carbon and anode on the performance of direct carbon solid oxide fuel cells. Solid State Ionics, 2019, 343, 115127.	1.3	19
500	One-pot synthesis of SnS/C nanocomposites on carbon paper as a high-performance free-standing anode for lithium ion batteries. Journal of Alloys and Compounds, 2019, 779, 67-73.	2.8	19
501	Achievement of a polymer-free KAc gel electrolyte for advanced aqueous K-Ion battery. Energy Storage Materials, 2021, 41, 133-140.	9.5	19
502	Structure, microstructure and transport properties of mixed ionic-electronic conductors based on bismuth oxide Part I. Bi-Y-Cu-O system. Solid State Ionics, 1994, 72, 209-217.	1.3	18
503	Removal of Hydrogen Sulfide from a Fuel Gas Stream by Electrochemical Membrane Separation. Journal of the Electrochemical Society, 2002, 149, D160.	1.3	18
504	Self-assembly of cerium compound nanopetals via a hydrothermal process: Synthesis, formation mechanism and properties. Journal of Solid State Chemistry, 2006, 179, 1733-1738.	1.4	18

#	Article	IF	CITATIONS
505	High performance solid oxide fuel cells based on tri-layer yttria-stabilized zirconia by low temperature sintering process. Journal of Power Sources, 2010, 195, 7230-7233.	4.0	18
506	Solid Oxide Fuel Cells. , 2012, , 7-36.		18
507	A Durable Electrode for Solid Oxide Cells: Mesoporous Ce0.8Sm0.2O1.9 Scaffolds Infiltrated with a Sm0.5Sr0.5CoO3-δCatalyst. Electrochimica Acta, 2017, 235, 646-653.	2.6	18
508	An extremely active and durable Mo 2 C/graphene-like carbon based electrocatalyst for hydrogen evolution reaction. Materials Today Energy, 2017, 6, 230-237.	2.5	18
509	From Checkerboardâ€Like Sand Barriers to 3D Cu@CNF Composite Current Collectors for Highâ€Performance Batteries. Advanced Science, 2018, 5, 1800031.	5.6	18
510	Template synthesis of carbon-coated Co9S8 composite with largely improved capacity for lithium ion batteries. Materials Letters, 2018, 217, 163-166.	1.3	18
511	A bi-functional WO3-based anode enables both energy storage and conversion in an intermediate-temperature fuel cell. Energy Storage Materials, 2018, 12, 79-84.	9.5	18
512	Structural Insight into the Abnormal Capacity of a Co-Substituted Tunnel-Type Na _{0.44} MnO ₂ Cathode for Sodium-Ion Batteries. ACS Applied Materials & Interfaces, 2020, 12, 47548-47555.	4.0	18
513	Enhanced Performance of La _{0.6} Sr _{0.4} Co _{0.2} Fe _{0.8} O _{3-delta} (LSCF) Cathodes with Graded Microstructure Fabricated by Tape Casting. Journal of Electrochemical Science and Technology. 2010. 1, 50-56.	0.9	18
514	Preparation of Ordered Macroporous Sr0.5Sm0.5CoO3as Cathode for Solid Oxide Fuel Cells. Chemistry Letters, 2001, 30, 1032-1033.	0.7	17
515	Nanostructured metallic foam electrodeposits on a nonconductive substrate. Journal of Materials Chemistry, 2012, 22, 1028-1032.	6.7	17
516	Application of high velocity oxygen fuel flame (HVOF) spraying toÂfabrication of La0.8Sr0.2Ga0.8Mg0.2O3 electrolyte for solid oxide fuelÂcells. Journal of Power Sources, 2016, 301, 62-71.	4.0	17
517	A direct carbon solid oxide fuel cell stack on a single electrolyte plate fabricated by tape casting technique. Journal of Alloys and Compounds, 2019, 794, 294-302.	2.8	17
518	Simple and Cost-Effective Approach To Dramatically Enhance the Durability and Capability of a Layered δ-MnO ₂ Based Electrode for Pseudocapacitors: A Practical Electrochemical Test and Mechanistic Revealing. ACS Applied Energy Materials, 2019, 2, 2743-2750.	2.5	17
519	Solvothermal alcoholysis synthesis of hierarchically porous TiO2-carbon tubular composites as high-performance anodes for lithium-ion batteries. Electrochimica Acta, 2019, 308, 253-262.	2.6	17
520	Unraveling the Mechanism of Water-Mediated Sulfur Tolerance via Operando Surface-Enhanced Raman Spectroscopy. ACS Applied Materials & Interfaces, 2020, 12, 2370-2379.	4.0	17
521	Facile Room-Temperature Synthesis of a Highly Active and Robust Single-Crystal Pt Multipod Catalyst for Oxygen Reduction Reaction. ACS Applied Materials & Interfaces, 2020, 12, 49510-49518.	4.0	17
522	Construction of heterostructured NiFe ₂ O ₄ -C nanorods by transition metal recycling from simulated electroplating sludge leaching solution for high performance lithium ion batteries. Nanoscale, 2020, 12, 13398-13406.	2.8	17

#	Article	IF	CITATIONS
523	Novel Cu(Zn)–Ge–P compounds as advanced anode materials for Li-ion batteries. Energy and Environmental Science, 2021, 14, 2394-2407.	15.6	17
524	Preparation of mesoporous yttria-stabilized zirconia (YSZ) and YSZ–NiO using a triblock copolymer as surfactant. Journal of Materials Chemistry, 2000, 10, 2603-2605.	6.7	16
525	Effect of Pd Coating on Hydrogen Permeation of Ni-Barium Cerate Mixed Conductor. Electrochemical and Solid-State Letters, 2002, 5, J5.	2.2	16
526	Protons crossing triple phase boundaries based on a metal catalyst, Pd or Ni, and barium zirconate. Physical Chemistry Chemical Physics, 2013, 15, 12525.	1.3	16
527	Highly Efficient Layer-by-Layer-Assisted Infiltration for High-Performance and Cost-Effective Fabrication of Nanoelectrodes. ACS Applied Materials & Interfaces, 2014, 6, 17352-17357.	4.0	16
528	A Facile and Environmentally Friendly One-Pot Synthesis of Pt Surface-Enriched Pt-Pd(x)/C Catalyst for Oxygen Reduction. Electrocatalysis, 2018, 9, 495-504.	1.5	16
529	Synthesis of biomass-derived 3D porous graphene-like via direct solid-state transformation and its potential utilization in lithium-ion battery. Ionics, 2018, 24, 1879-1886.	1.2	16
530	Nd3+ ions induced rational morphology control of transition metal oxides for high energy storage performance. Journal of Power Sources, 2020, 472, 228599.	4.0	16
531	Protonic ceramic materials for clean and sustainable energy: advantages and challenges. International Materials Reviews, 2023, 68, 272-300.	9.4	16
532	The Performance of Two Phase Commit Protocols in the Presence of Site Failures. Distributed and Parallel Databases, 1998, 6, 157-182.	1.0	15
533	Electrochemical Properties of GeS2â€Based Glassâ€Polymer Composite Electrolytes for Lithiumâ€ion Batteries. Journal of the Electrochemical Society, 1998, 145, 1949-1952.	1.3	15
534	Porous Electrodes for Lowâ€Temperature Solid Oxide Fuel Cells Fabricated by a Combustion Spray Process. Journal of the American Ceramic Society, 2004, 87, 2139-2142.	1.9	15
535	Metalâ€Air Batteries: Metal–Air Batteries with High Energy Density: Li–Air versus Zn–Air (Adv. Energy) Tj E	TQ _Q 1 1 0. 10.2	784314 rg8T 15
536	Contribution of carbon fiber paper (CFP) to the capacitance of a CFP-supported manganese oxide supercapacitor. Journal of Power Sources, 2014, 248, 1197-1200.	4.0	15
537	<i>In-situ</i> transmission electron microscopy study of oxygen vacancy ordering and dislocation annihilation in undoped and Sm-doped CeO2 ceramics during redox processes. Journal of Applied Physics, 2016, 120, .	1.1	15
538	La2NiO4+δ Infiltration of Plasma-Sprayed LSCF Coating for Cathode Performance Improvement. Journal of Thermal Spray Technology, 2016, 25, 392-400.	1.6	15
539	Anode-supported solid oxide fuel cells based on Sm0.2Ce0.8O1.9 electrolyte fabricated by a phase-inversion and drop-coating process. International Journal of Hydrogen Energy, 2016, 41, 10907-10913.	3.8	15
540	Understanding the Impact of Sulfur Poisoning on the Methane-Reforming Activity of a Solid Oxide Fuel Cell Anode. ACS Catalysis, 2021, 11, 13556-13566.	5.5	15

#	Article	IF	CITATIONS
541	Creation of Porous Ceria by Sublimation of Tin Dioxide during Sintering. Advanced Engineering Materials, 2006, 8, 89-93.	1.6	14
542	Ordered ZnO Nanorods Synthesized by Combustion Chemical Vapor Deposition. Journal of Nanoscience and Nanotechnology, 2007, 7, 4529-4533.	0.9	14
543	Enhancing SOFC Electrode Performance Through Surface Modification. ECS Transactions, 2013, 57, 1801-1810.	0.3	14
544	Highly active Sm0.2Ce0.8O1.9 powders of very low apparent density derived from mixed cerium sources. Journal of Power Sources, 2013, 229, 277-284.	4.0	14
545	Sulfurization synthesis of a new anode material for Li-ion batteries: understanding the role of sulfurization in lithium ion conversion reactions and promoting lithium storage performance. Journal of Materials Chemistry A, 2019, 7, 21270-21279.	5.2	14
546	Zn(Cu)Si ₂₊ <i>_x</i> P ₃ Solid Solution Anodes for Highâ€Performance Liâ€Ion Batteries with Tunable Working Potentials. Advanced Functional Materials, 2019, 29, 1903638.	7.8	14
547	Targeted synthesis and reaction mechanism discussion of Mo ₂ C based insertion-type electrodes for advanced pseudocapacitors. Journal of Materials Chemistry A, 2020, 8, 7819-7827.	5.2	14
548	Surface enhanced performance of La0.6Sr0.4Co0.2Fe0.8O3-δ cathodes by infiltration Pr-Ni-Mn-O progress. Journal of Alloys and Compounds, 2022, 902, 163337.	2.8	14
549	Nanostructured and functionally graded cathodes for intermediate-temperature SOFCs. Fuel Cells Bulletin, 2004, 2004, 12-15.	0.7	13
550	Enhancing effect of DNA on chemiluminescence from the decomposition of hydrogen peroxide catalyzed by copper(II). Analytical and Bioanalytical Chemistry, 2005, 381, 828-832.	1.9	13
551	Diameter-dependent voltammetric properties of carbon nanotubes. Chemical Physics Letters, 2006, 418, 524-529.	1.2	13
552	Synthesis and characterization of robust, mesoporous electrodes for solid oxide fuel cells. Journal of Materials Chemistry A, 2016, 4, 7650-7657.	5.2	13
553	Fabrication of TiO ₂ coated porous CoMn ₂ O ₄ submicrospheres for advanced lithium-ion anodes. RSC Advances, 2017, 7, 21214-21220.	1.7	13
554	High rate and high capacity lithiation of rGO-coated Co2(OH)2CO3 nanosheet arrays for lithium-ion batteries through the involvement of CO32â^'. Electrochimica Acta, 2017, 235, 98-106.	2.6	13
555	Co-polymerization of polysilicic-zirconium with enhanced coagulation properties for water purification. Separation and Purification Technology, 2018, 200, 59-67.	3.9	13
556	Achieving Durable and Fast Charge Storage of MoO2-Based Insertion-Type Pseudocapacitive Electrodes via N-Doped Carbon Coating . ACS Sustainable Chemistry and Engineering, 2020, 8, 2806-2813.	3.2	13
557	A Nonstoichiometric Niobium Oxide/Graphite Composite for Fastâ€Charge Lithiumâ€lon Batteries. Small, 2022, 18, .	5.2	13
558	Nondestructive volumetric 3-D chemical mapping of nickel-sulfur compounds at the nanoscale. Nanoscale, 2012, 4, 1557.	2.8	12

#	Article	IF	CITATIONS
559	BaZr 0.9 Yb 0.1 O 3â^î´-modified bi-electrode supported solid oxide fuel cells with enhanced coking and sulfur tolerance. Journal of Power Sources, 2013, 243, 24-28.	4.0	12
560	Enhanced capacitive performance of nickel oxide on porous LaO·7SrO·3CoO3-δ ceramic substrate for electrochemical capacitors. International Journal of Hydrogen Energy, 2018, 43, 19589-19599.	3.8	12
561	Energy minimization for heterogeneous wireless sensor networks. Journal of Embedded Computing, 2009, 3, 109-117.	0.2	11
562	Controlling grain size in columnar YSZ coating formation by droplet filtering assisted PS-PVD processing. RSC Advances, 2015, 5, 102126-102133.	1.7	11
563	Aerosol sprayed Mn 1.5 Co 1.5 O 4 protective coatings for metallic interconnect of solid oxide fuel cells. International Journal of Hydrogen Energy, 2016, 41, 20305-20313.	3.8	11
564	Fast Oxygen Transport in Bottlelike Channels for Y-Doped BaZrO3: A Reactive Molecular Dynamics Investigation. Journal of Physical Chemistry C, 2019, 123, 25611-25617.	1.5	11
565	Lattice Boltzmann modelling of the coupling between charge transport and electrochemical reactions in a solid oxide fuel cell with a patterned anode. International Journal of Hydrogen Energy, 2019, 44, 30293-30305.	3.8	11
566	Mono-disperse PdO nanoparticles prepared via microwave-assisted thermo-hydrolyzation with unexpectedly high activity for formic acid oxidation. Electrochimica Acta, 2020, 329, 135166.	2.6	11
567	Considerations in design and characterization of solid-state electrochemical systems. Solid State lonics, 1992, 52, 3-13.	1.3	10
568	General loop fusion technique for nested loops considering timing and code size. , 2004, , .		10
569	Oxygen ion transference number of doped lanthanum gallate. Journal of Power Sources, 2008, 185, 917-921.	4.0	10
570	Unbiased characterization of three-phase microstructure of porous lanthanum doped strontium manganite/yttria-stabilized zirconia composite cathodes for solid oxide fuel cells using atomic force microscopy and stereology. Journal of Power Sources, 2009, 192, 367-371.	4.0	10
571	Sheet Resistance in Thin Film Solid Oxide Fuel Cell Model Cathodes: A Case Study on Circular Bi1-xSrxFeO3-Â Microelectrodes. ECS Transactions, 2012, 45, 213-224.	0.3	10
572	Electrostatic Force Microscopic Characterization of Early Stage Carbon Deposition on Nickel Anodes in Solid Oxide Fuel Cells. Nano Letters, 2015, 15, 6047-6050.	4.5	10
573	Interfacial effects on electrical conductivity in ultrafine-grained Sm0.2Ce0.8O2â^'î´ electrolytes fabricated by a two-step sintering process. International Journal of Hydrogen Energy, 2017, 42, 11823-11829.	3.8	10
574	Domain structures and Prco antisite point defects in double-perovskite PrBaCo2O5+δ and PrBa0.8Ca0.2Co2O5+δ. Ultramicroscopy, 2018, 193, 64-70.	0.8	10
575	Precision surface modification of solid oxide fuel cells <i>via</i> layer-by-layer surface sol–gel deposition. Journal of Materials Chemistry A, 2022, 10, 8798-8806.	5.2	10
576	Chemical Stability of Sodium Beta″â€Alumina Electrolyte in Sulfur/Sodium Polysulfide Melts. Journal of the Electrochemical Society, 1988, 135, 741-749.	1.3	9

#	Article	IF	CITATIONS
577	Probing Water Interactions and Vacancy Production on Gadolinia-Doped Ceria Surfaces Using Electron Stimulated Desorption. Journal of Physical Chemistry B, 2005, 109, 11257-11262.	1.2	9
578	Design optimization and space minimization considering timing and code size via retiming and unfolding. Microprocessors and Microsystems, 2006, 30, 173-183.	1.8	9
579	A durable polyvinyl butyral-CsH2PO4 composite electrolyte for solid acid fuel cells. Journal of Power Sources, 2017, 359, 1-6.	4.0	9
580	Significantly enhanced electrochemical performance of a ZnCo ₂ O ₄ anode in a carbonate based electrolyte with fluoroethylene carbonate. RSC Advances, 2017, 7, 18491-18499.	1.7	9
581	Achievement of high energy carbon based supercapacitors in acid solution enabled by the balance of SSA with abundant micropores and conductivity. Electrochimica Acta, 2020, 353, 136562.	2.6	9
582	Organic Macromolecule regulated the structure of vanadium oxide with high capacity and stability for aqueous Zinc-ion batteries. Applied Surface Science, 2022, 592, 153295.	3.1	9
583	Characterization of the fission yeast ribosomal DNA binding factor: components share homology with Upstream Activating Factor and with SWI/SNF subunits. Nucleic Acids Research, 2002, 30, 5347-5359.	6.5	8
584	Charging effects on electron-stimulated desorption of cations from gadolinia-doped ceria surfaces. Applied Surface Science, 2005, 243, 166-177.	3.1	8
585	Modeling of patterned mixed-conducting electrodes and the importance of sheet resistance at small feature sizes. Solid State Ionics, 2007, 178, 249-252.	1.3	8
586	Graphene for ultracapacitors. , 2010, , .		8
587	Resonant surface enhancement of Raman scattering of Ag nanoparticles on silicon substrates fabricated by dc sputtering. Journal of Vacuum Science and Technology A: Vacuum, Surfaces and Films, 2012, 30, .	0.9	8
588	Growth and characterization of La0.85Sr0.15MnO3 thin films for fuel cell applications. Applied Surface Science, 2012, 258, 6199-6203.	3.1	8
589	Enhancement of Electrochemical Properties, Impedance and Resistances of Microâ€ŧubular IT‧OFCs with Novel Asymmetric Structure Based on BaZr 0.1 Ce 0.7 Y 0.1 Yb 0.1 O 3â^' δ Proton Conducting Electrolyte. Fuel Cells, 2020, 20, 70-79.	1.5	8
590	Four probe polarization techniques and the application to investigations of solid-state electrochemical devices. Electrochimica Acta, 1993, 38, 1289-1300.	2.6	7
591	Properties and morphology of doped polycrystalline Na-β″-alumina electrolytes. Solid State Ionics, 1993, 62, 185-191.	1.3	7
592	Sulfur-Tolerant Cathode Materials in Electrochemical Membrane System for H[sub 2]S Removal from Hot Fuel Gas. Journal of the Electrochemical Society, 2004, 151, D55.	1.3	7
593	Noble Metal Nanostructures Synthesized inside Mesoporous Nanotemplate Pores. Electrochemical and Solid-State Letters, 2004, 7, J17.	2.2	7
594	Modeling Electrophoretic Deposition on Porous Nonâ€Conducting Substrates Using Statistical Design of Experiments. Journal of the American Ceramic Society, 2006, 89, 2787-2795.	1.9	7

#	Article	IF	CITATIONS
595	Fabrication and characterization of hermetic solid oxide fuel cells without sealant. Solid State Ionics, 2006, 177, 367-375.	1.3	7
596	Optimizing Address Assignment and Scheduling for DSPs With Multiple Functional Units. IEEE Transactions on Circuits and Systems Part 2: Express Briefs, 2006, 53, 976-980.	2.3	7
597	Promising Ni–Fe–LSGMC anode compatible with lanthanum gallate electrolyte. Electrochimica Acta, 2009, 54, 3872-3876.	2.6	7
598	Understanding the phase formation and compositions of barium carbonate modified NiO-yttria stabilized zirconia for fuel cell applications. International Journal of Hydrogen Energy, 2015, 40, 15597-15604.	3.8	7
599	High performance intermediate temperature solid oxide fuel cells with Ba0.5Sr0.5Co0.8Fe0.1Nb0.1O3â^'δ as cathode. Ceramics International, 2016, 42, 19397-19401.	2.3	7
600	Liquid plasma sprayed nano-network La0.4Sr0.6Co0.2Fe0.8O3/Ce0.8Gd0.2O2 composite as a high-performance cathode for intermediate-temperature solid oxide fuel cells. Journal of Power Sources, 2016, 327, 622-628.	4.0	7
601	Oxygen Defect Engineering: Improving the Activity for Oxygen Evolution Reaction by Tailoring Oxygen Defects in Double Perovskite Oxides (Adv. Funct. Mater. 34/2019). Advanced Functional Materials, 2019, 29, 1970236.	7.8	7
602	Bimetal Metalâ€Organic Frameworks Derived Hierarchical Porous Cobalt@Nitrogenâ€Doped Carbon Tubes as An Efficient Electrocatalyst for Oxygen Reduction Reaction. ChemElectroChem, 2022, 9, .	1.7	7
603	BaCuGd2 O 5 â€â€‰BaCeO3 Composite Cathodes for Barium Cerateâ€Based Electrolytes. Journal e Electrochemical Society, 1997, 144, 4049-4053.	of the	6
604	Effects of stable fish oil and simvastatin on plasma lipoproteins in patients with hyperlipidemia. Nutrition Research, 2003, 23, 1027-1034.	1.3	6
605	Iterational retiming. , 2005, , .		6
606	Gd2Ti2-XMoXO7-Based Anode Materials for H2S-Air Solid Oxide Fuel Cells. ECS Transactions, 2006, 1, 293-302.	0.3	6
607	Detecting Link Communities Based on Local Approach. , 2011, , .		6
608	First-principles study of hydrogen permeation in palladium-gold alloys. Applied Physics Letters, 2011, 99, 181901.	1.5	6
609	Rational Design of Sulfur-Tolerant Anode Materials for Solid Oxide Fuel Cells. ECS Transactions, 2013, 58, 217-229.	0.3	6
610	Hydrogen oxidation at the Pt–BaZr0.1Ce0.7Y0.1Yb0.1O3â^'δ (BZCYYb) interface. Physical Chemistry Chemical Physics, 2013, 15, 3820.	1.3	6
611	Phase and Morphology Evolution Induced Lithium Storage Capacity Enhancement of Porous CoO Nanowires Intertwined with Reduced Graphene Oxide Nanosheets. ChemElectroChem, 2018, 5, 3679-3687.	1.7	6
612	Highly Efficient CO ₂ Utilization via Aqueous Zinc– or Aluminum–CO ₂ Systems for Hydrogen Gas Evolution and Electricity Production. Angewandte Chemie, 2019, 131, 9606-9611.	1.6	6

#	Article	IF	CITATIONS
613	Promoting photocatalytic hydrogen evolution over the perovskite oxide Pr _{0.5} (Ba _{0.5} Sr _{0.5}) _{0.5} Co _{0.8} Fe _{0.2} Co by plasmon-induced hot electron injection. Nanoscale, 2020, 12, 18710-18720.	/>S <aub>3<!--</td--><td>sub></td></aub>	sub>
614	Evaluation of the Volumetric Activity of the Air Electrode in a Zinc–Air Battery Using a Nitrogen and Sulfur Co-doped Metal-free Electrocatalyst. ACS Applied Materials & Interfaces, 2020, 12, 57064-57070.	4.0	6
615	Preparation of mesoporous La0.85Sr0.15MnO3 using a surfactant-templated sol-gel process. Journal of Materials Science Letters, 2000, 19, 1473-1476.	0.5	5
616	Transport and surface properties of Sr0.25Bi0.5FeO3â^´Î´ mixed conductor. Solid State Ionics, 2002, 149, 299-307.	1.3	5
617	Highly Efficient Electron Stimulated Desorption of O+from Gadolinia-Doped Ceria Surfaces. Journal of Physical Chemistry B, 2006, 110, 10779-10784.	1.2	5
618	Investigation into the diffusion and oxidation behavior of the interface between a plasma-sprayed anode and a porous steel support for solid oxide fuel cells. Journal of Power Sources, 2016, 323, 1-7.	4.0	5
619	Voltage Assignment and Loop Scheduling for Energy Minimization while Satisfying Timing Constraint with Guaranteed Probability. , 2006, , .		4
620	Loop scheduling with complete memory latency hiding on multi-core architecture. , 2006, , .		4
621	Microarchitectured solid oxide fuel cells with improved energy efficiency (Part II): Fabrication and characterization. Journal of Power Sources, 2015, 293, 883-891.	4.0	4
622	High pressure structural study of samarium doped CeO2 oxygen vacancy conductor — Insight into the dopant concentration relationship to the strain effect in thin film ionic conductors. Solid State lonics, 2016, 292, 59-65.	1.3	4
623	In situ Raman spectroscopic analysis of the coking resistance mechanism on SrZr0.95Y0.05O3â^'x surface for solid oxide fuel cell anodes. Journal of Power Sources, 2016, 324, 282-287.	4.0	4
624	Loop Distribution and Fusion with Timing and Code Size Optimization for Embedded DSPs. Lecture Notes in Computer Science, 2005, , 121-130.	1.0	4
625	Generation of highly porous Li‒Mg and Li‒Zn alloys from kinetically controlled lithiation. The Philosophical Magazine: Physics of Condensed Matter B, Statistical Mechanics, Electronic, Optical and Magnetic Properties, 2001, 81, 119-131.	0.6	3
626	Electrocatalytic properties of an Sr0.25Bi0.5FeO3–Î′/LSGM interface. Journal of Solid State Electrochemistry, 2001, 5, 375-381.	1.2	3
627	Variable Length Pattern Matching for Hardware Network Intrusion Detection System. Journal of Signal Processing Systems, 2010, 59, 85-93.	1.4	3
628	Sodium Ion Batteries: A New rGOâ€Overcoated Sb ₂ Se ₃ Nanorods Anode for Na ⁺ Battery: In Situ Xâ€Ray Diffraction Study on a Live Sodiation/Desodiation Process (Adv.) Tj ETQo	07080 rgB	T ‡Overlock I

629	A-MapCG: An Adaptive MapReduce Framework for GPUs. , 2017, , .		3
630	Cobalt Oxide Nanorods Prepared by a Template-Free Method for Lithium Battery Application. Journal of Electrochemical Science and Technology, 2016, 7, 206-213.	0.9	3

#	Article	IF	CITATIONS
631	Effect of geometry and interfacial resistance on current distribution and energy dissipation at metal/superconductor junctions. Journal of Materials Research, 1989, 4, 530-538.	1.2	2
632	Assignment and scheduling of real-time dsp applications for heterogeneous functional units. , 0, , .		2
633	Loop Distribution and Fusion with Timing and Code Size Optimization. Journal of Signal Processing Systems, 2011, 62, 325-340.	1.4	2
634	Probing and Mapping Electrode Surfaces in Solid Oxide Fuel Cells. Journal of Visualized Experiments, 2012, , e50161.	0.2	2
635	Enhanced density of sol–gel derived La0.8S0.2MnO3 thin film with an electric field assisted deposition. Materials Letters, 2013, 92, 192-194.	1.3	2
636	Rational design of Nb-based alloys for hydrogen separation: A first principles study. AIP Advances, 2013, 3, .	0.6	2
637	LSRB-CSR: A Low Overhead Storage Format for SpMV on the GPU Systems. , 2015, , .		2
638	Compile-Time Automatic Synchronization Insertion and Redundant Synchronization Elimination for GPU Kernels. , 2016, , .		2
639	Template-Free Synthesis of Tin Oxides with a Dual Pore Structure. Electrochimica Acta, 2016, 200, 90-96.	2.6	2
640	(Invited) Robust and Active Mixed-Conducting Electrodes for Intermediate-Temperature Fuel Cells. ECS Transactions, 2017, 80, 3-12.	0.3	2
641	Simultaneous-shot inversion for PDE-constrained optimization problems with missing data. Inverse Problems, 2019, 35, 025003.	1.0	2
642	Hierarchical hollow microspheres of carbon nanorods with enhanced supercapacitor performance. Materials Today Communications, 2021, 28, 102500.	0.9	2
643	A Direct Carbon Solid Oxide Fuel Cell Stack Based on a Single Electrolyte Plate Fabricated by Tape Casting Technique. Wuji Cailiao Xuebao/Journal of Inorganic Materials, 2019, 34, 509.	0.6	2
644	Electrical Performance of Ag-Based Ceramic Composite Electrodes and Their Application in Solid Oxide Fuel Cells. Wuli Huaxue Xuebao/ Acta Physico - Chimica Sinica, 2016, 32, 503-509.	2.2	2
645	Triple-Phase Boundaries (TPBs) in Fuel Cells and Electrolyzers. , 2022, , 299-328.		2
646	In Situ Characterization of Interfacial and Bulk Properties of Lithium Polymer Batteries Using 4-Probe DC Techniques. Materials Research Society Symposia Proceedings, 1992, 293, 107.	0.1	1
647	In-Situ Characterization of Electrode Reactions in Solid Oxide Fuel Cells. ECS Proceedings Volumes, 2003, 2003-07, 1132-1146.	0.1	1
648	Switching-activity minimization on instruction-level loop scheduling for VLIW DSP applications. , 0, , .		1

#	Article	IF	CITATIONS
649	Maximum Loop Distribution and Fusion for Two-level Loops Considering Code Size. , 0, , .		1
650	Porous SOFC Anodes Prepared by Sublimation of an Immiscible Metal Oxide during Sintering. Electrochemical and Solid-State Letters, 2006, 9, B25.	2.2	1
651	FTIR STUDY OF THE OXYGEN REDUCTION REACTIONS ON Sm _{0.5} Sr _{0.5} CoO ₃ . Surface Review and Letters, 2007, 14, 587-591.	0.5	1
652	Electron stimulated desorption of O2+ from gadolinia-doped ceria surfaces. Applied Surface Science, 2008, 254, 4965-4969.	3.1	1
653	Overlapping Community Detection via Leader-Based Local Expansion in Social Networks. , 2012, , .		1
654	4 Preparation of Hierarchical (Nano/Meso/Macro) Porous Structures Using Electrochemical Deposition. Modern Aspects of Electrochemistry, 2012, , 297-330.	0.2	1
655	Stability and Performance of Silver in an SOFC Interconnect Environment. , 0, , 301-312.		1
656	A Novel Porous Electronic Conducting Ceramics Loaded with Silver Nano Particles as Cathode for Zinc-Air Batteries. Wuji Cailiao Xuebao/Journal of Inorganic Materials, 2018, 33, 854.	0.6	1
657	Effect of Surface Modification on Catalytic Properties of Sr[sub 0.25]Bi[sub 0.5]FeO[sub 3â~Î] Membranes. Electrochemical and Solid-State Letters, 1999, 2, 452.	2.2	Ο
658	The Investigation on Au Nano-particles on Si Wafer after Annealing at Different Temperatures. , 2010, , .		0
659	The Role of Sulfur in the Porous Cermet Solid Oxide Fuel Cell Anode Microstructure. , 2012, , .		Ο
660			0
661	Raman Spectroscopy Study of SOFC Electrode Surfaces. ECS Transactions, 2013, 57, 1437-1444.	0.3	0
662	Energetics of Protonic Species in Yttrium-doped Barium Zirconate: A Density Functional Theory Study. Materials Research Society Symposia Proceedings, 2013, 1495, 1.	0.1	0
663	An Optimized GP-GPU Warp Scheduling Algorithm for Sparse Matrix-Vector Multiplication. , 2013, , .		0
664	Graphene-Encapsulated Nanosheet-Assembled Zinc-Nickel-Cobalt Oxide Microspheres for Enhanced Lithium Storage. ChemSusChem, 2016, 9, 128-128.	3.6	0
665	In-situ Transmission Electron Microscopy Study of Oxygen Vacancy Ordering and Dislocation Annihilation in Undoped and Sm-doped CeO2 Ceramics During Redox Processes. Microscopy and Microanalysis, 2017, 23, 1626-1627.	0.2	0
666	Toward a New Generation of Intermediate-Temperature Fuel Cells. ECS Transactions, 2017, 78, 1821-1829.	0.3	0

#	Article	IF	CITATIONS
667	Batteries: From Checkerboard-Like Sand Barriers to 3D Cu@CNF Composite Current Collectors for High-Performance Batteries (Adv. Sci. 7/2018). Advanced Science, 2018, 5, 1870040.	5.6	0
668	Fast Document Cosine Similarity Self-Join on GPUs. , 2018, , .		0
669	Domain Structures and PrCo Antisite Point Defects in Double-perovskite PrBaCo2O5+δ. Microscopy and Microanalysis, 2019, 25, 2016-2017.	0.2	0
670	Modeling of MIEC Cathodes: The Effect of Sheet Resistance. Ceramic Engineering and Science Proceedings, 0, , 153-160.	0.1	0
671	Fabrication and Characterization of Dense La0.85.Sr0.15MnO3-Ce0.9Gd0.1O1.95 Composite Electrodes. , 0, , 177-182.		0
672	Examining Effects of Sulfur Poisoning on Ni/YSZ Solid Oxide Fuel Cell Anodes Using Synchrotron-Based X-Ray Imaging Techniques. , 2013, , .		0
673	Graphene-Wrapped Fe3O4 Anode Material for High-Performance Lithium Ion Batteries. , 2015, , .		0
674	Noble metal distribution in mesoporous silica as a selective active filter for semiconductor gas sensors. , 2018, , 433-436.		0
675	Activating the oxygen electrocatalytic activity of layer-structured Ca _{0.5} CoO ₂ nanofibers by iron doping. Dalton Transactions, 2022, 51, 3636-3641.	1.6	0
676	Dislocation-Pipe Diffusion of Protons in Hydrated Yttrium-Doped Barium Zirconate Simulated by Reactive Molecular Dynamics. ACS Applied Energy Materials, 2022, 5, 7269-7276.	2.5	0